Evaluation of leaf-to-canopy upscaling methodologies against carbon flux data in North America

Michael Sprintsin,[1,2] Jing M. Chen,[1] Ankur Desai,[3] and Christopher M. Gough[4]

Received 23 April 2010; revised 21 December 2011; accepted 22 December 2011; published 29 February 2012.

[1] Despite the wide acceptance of the "big-leaf" upscaling strategy in evapotranspiration modeling (e.g., the Penman-Monteith model), its usefulness in simulating canopy photosynthesis may be limited by the underlying assumption of homogeneous response of carbon assimilation light-response kinetics through the canopy. While previous studies have shown that the separation of the canopy into sunlit and shaded parts (i.e., two-leaf model) is typically more effective than big-leaf models for upscaling photosynthesis from leaf to canopy, a systematic comparison between these two upscaling strategies among multiple ecosystems has not been presented. In this study, gross primary productivity was modeled using two-leaf and big-leaf upscaling approaches in the Boreal Ecosystem Productivity Simulator for shrublands, broadleaf, and conifer forest types. When given the same leaf-level photosynthetic parameters, the big-leaf approach significantly underestimated canopy-level GPP while the two-leaf approach more closely predicted both the magnitude and day-to-day variability in eddy covariance measurements. The underestimation by the big-leaf approach is mostly caused by its exclusion of the photosynthetic contributions of shaded leaves. Tests of the model sensitivity to a foliage clumping index revealed that the contribution of shaded leaves to the total simulated productivity can be as high as 70% for highly clumped stands and seldom decreases below ~40% for less-clumped canopies. Our results indicate that accurate upscaling of photosynthesis across a broad array of ecosystems requires an accurate description of canopy structure in ecosystem models.

Citation: Sprintsin, M., J. M. Chen, A. Desai, and C. M. Gough (2012), Evaluation of leaf-to-canopy upscaling methodologies against carbon flux data in North America, *J. Geophys. Res.*, *117*, G01023, doi:10.1029/2010JG001407.

1. Introduction

[2] Traditionally, many ecosystem models have used a simple light-use efficiency [*Monteith*, 1972, 1973] approach to estimate photosynthetic carbon assimilation by plant canopies (gross primary production (GPP)). Since the advent of the process-based "Farquhar" formulation of leaf photosynthesis [*Farquhar et al.*, 1980], many ecosystem models have adopted this leaf-level model as a basis to upscale to the canopy, with some approaches assuming common physiological parameters throughout the canopy while others partition the canopy into different layers with distinct light-response features. Consequently, canopy-level GPP estimation offers a choice of leaf-to-canopy upscaling methodologies, with the approach potentially affecting the outcome of GPP simulations [e.g., *Wang and Leuning*, 1998; *Dai et al.*, 2004; *Liu et al.*, 1997; *Chen et al.*, 1999].

[3] The simplest of these upscaling methodologies is the "big-leaf" approach, which assumes that canopy carbon fluxes have the same relative responses to the environment as any single unshaded leaf on a canopy top [*Sellers et al.*, 1992; *Dai et al.*, 2004]. The applicability of a big-leaf approach [e.g., *Kull and Jarvis*, 1995; *Friend et al.*, 1997] is justified by the assumptions that within canopies, photosynthetic capacity, primarily reflected in leaf nitrogen content, is distributed in proportion to the profile of radiation [*de Pury and Farquhar*, 1997].

[4] Despite its wide acceptance for modeling evapotranspiration at different spatial scales [*Raupach and Finnigan*, 1988; *Moran et al.*, 1996; *Samson and Lemeur*, 2001; *Weiß and Menzel*, 2008], subsequent theoretical and experimental developments [*de Pury and Farquhar*, 1997; *Carswell et al.*, 2000; *Lai et al.*, 2000; *Meir et al.*, 2002] have brought into question assumptions behind the big-leaf approach in modeling vegetation productivity. It is well accepted in recent literature [e.g., *Friend*, 2001] that under realistic conditions, photosynthesis of most leaves is usually not light saturated and that, because of complex canopy architecture,

[1]Department of Geography, University of Toronto, Toronto, Ontario, Canada.
[2]Now at the Institute of Agricultural Engineering, Agricultural Research Organization Volcani Centre, Bet Dagan, Israel.
[3]Center for Climatic Research, Nelson Institute for Environmental Studies, University of Wisconsin – Madison, Madison, Wisconsin, USA.
[4]Department of Biology, Virginia Commonwealth University, Richmond, Virginia, USA.

0148-0227/12/2010JG001407

the distribution of absorbed irradiance is highly variable and does not necessarily follow Beer's law for one-dimensional (1-D) canopy radiative transfer as assumed for the single leaf. These findings challenge the assumption that photosynthetic capacity is solely proportional to absorbed irradiance. Additionally, since total canopy nitrogen may greatly exceed that of a single leaf upscaled using the big-leaf approach, total photosynthesis of a canopy (which is correlated to total canopy nitrogen) may be higher than that derived from a single upscaled leaf [*Kull*, 2002], leading to an inadequate simulation of CO_2 assimilation at the canopy level and to a consequent underestimation of GPP by big-leaf models.

[5] While the most advanced radiative transfer algorithms developed for fine-scale (e.g., site-level) applications have improved on big-leaf models by relying on a computationally intensive radiative transfer code, there is a need for an intermediate approach that can be generalized for regional to global ecosystem modeling, where computational efficiency is paramount. A simpler sunlit-shaded leaf separation approach, within which the vegetation is treated as two big leaves under different illumination conditions, was proposed more than three decades ago [*Sinclair et al.*, 1976] and has been continuously investigated since then [*de Pury and Farquhar*, 1997; *Wang and Leuning*, 1998; *Chen et al.*, 1999; *Mercado et al.*, 2006]. Two-leaf models have been successfully tested for applications at local and regional scales and have been found to sufficiently capture much of the variation present in complex multilayered sunlit-shaded leaf separation approaches [e.g., *Kotchenova et al.*, 2004] in a way that the big-leaf upscaling cannot achieve [*de Pury and Farquhar*, 1997; *Chen et al.*, 1999; *Dai et al.*, 2004; *Mercado et al.*, 2006, 2007].

[6] Although the underestimation of GPP by the big-leaf approach could be improved by site-level tuning of photosynthetic parameters [e.g., *Lloyd et al.*, 1995], such computationally intensive parameterization loses global-scale applicability. Thus, we focus here on the performance of big-leaf and two-leaf models when using the same leaf-level parameterization for several land-cover types across large latitudinal ranges. Direct comparisons of the two upscaling approaches at multiple sites have not been done to our knowledge. Given the still relatively common use of the big-leaf models (and its simplified formulation of light-use efficiency models) and the plethora of data now available for evaluation from the global network of flux towers, it is prudent to reevaluate how well two-leaf and big-leaf approaches simulate GPP and how the differences between both are sensitive to site land cover and location.

[7] There are ecophysiological reasons to suspect that big-leaf models are likely to poorly simulate canopy GPP. First, photosynthesis of C_3 plants is largely limited by the drawdown in CO_2 concentrations from the atmosphere to the sites of carboxylation. Two steps dominate the pathway of CO_2. The first is diffusion of CO_2 from the atmosphere to substomatal cavities via the stomata. The second is its diffusion from the substomatal cavities to the sites of carboxylation via leaf mesophyll. The conductance inside the leaf mesophyll (also known as internal conductance) has been traditionally assumed infinite and therefore nonlimiting for photosynthesis. Recent evidence, however, points to mesophyll conductance that can be finite and highly variable [*Flexas et al.*, 2008; *Warren*, 2008], suggesting that the diffusion from substomatal cavities to sites of carboxylation is at least as large a limitation of photosynthesis as stomata [*Warren*, 2008]. As formulated, the big-leaf approach scales only stomatal conductance [*Sellers et al.*, 1992] while leaf internal regulation remains unchanged no matter how many layers of leaves are operating simultaneously (i.e., internal conductances are in parallel in reality). Such a way of scaling may lead to misinterpretation of the physiological mechanism of CO_2 assimilation because one (i.e., big) leaf has only one mesophyll conductance. In reality, several layers of leaves operate simultaneous in assimilating CO_2 from the atmosphere, meaning that several internal leaf conductances operate in parallel. As the mesophyll conductance to CO_2 transfer is different in shaded and in sunlit leaves [*Piel et al.*, 2002], a two-leaf approach avoids these drawbacks, accounting for the role of shaded leaves in the canopy-level photosynthesis, which averts the amplification of leaf internal control of the CO_2 flow (i.e., too-small overall internal conductance) as imposed by the big-leaf model.

[8] Second, the two-leaf representation is able to apply the separation of incoming radiation into its direct and diffuse portions. Sunlit leaf irradiance and shaded leaf irradiance are important variables because the penetrations of direct and diffuse radiation into the canopy vary [*Weiss and Norman*, 1985] and because they may have different effects on stomatal conductance and electron transport rate [*Chen et al.*, 1999]. Therefore, as was stated by *Norman* [1980, p. 65]: "the failure to differentiate between diffuse beam and direct radiation within the canopy can lead to erroneous calculations of photosynthesis."

[9] Although in the two-leaf approach, the shaded leaf receives only diffuse light (while the sunlit one receives both direct and diffuse radiation [*Spitters*, 1986]), the diffuse portion is used much more efficiently for photosynthesis than direct radiation. *Dai et al.* [2004, Figure 5] show, for example, that the shaded part of the canopy can absorb most of the diffuse component of the incoming photosynthetically active radiation (PAR), actually leading to the increase of assimilation in changing from a very clear to overcast sky. *Mercado et al.* [2006, Figure 5] demonstrated that the big-leaf approach is unresponsive to variation in diffuse irradiance, which likely leads to an underestimation of the total canopy photosynthesis. Thus, the assumption that a canopy can be represented as a single unshaded leaf on a canopy top makes the big-leaf approach insensitive to processes such as sunfleck penetration and diffuse radiation in the canopy. In this case, if canopy absorption of diffuse radiation for GPP is significant, a big-leaf model will underestimate the diurnal and day-to-day variations in canopy photosynthesis. While diurnal variability between the two models is worthwhile to investigate, the significant variation in radiation during the day will generally blur the differences between big-leaf and two-leaf models. Consequently, a worthwhile test of the appropriateness of the big-leaf approach would be to compare how well two-leaf and big-leaf models represent daily variations in GPP, even if GPP magnitude is poorly simulated, since the latter effect can be reduced with site-specific parameter tuning. Saying that, it should be kept in mind that this lack of day-to-day variability in GPP simulated by the big-leaf model is caused not only by its inability to reflect the radiation control on shaded leaf photosynthesis, as

analyzed above, but also by the amplified leaf internal resistance to the CO_2 flow imbedded in the big-leaf formulation, which also makes the model insensitive to driving factors affecting the canopy photosynthesis.

[10] Currently, there is a lack of systematic comparisons between two-leaf and big-leaf models at multiple field sites, leaving doubts on the suitability of either approach in the context of regional to global model simulations of GPP for multiple ecosystem types. Previous studies have shown the big-leaf approach to match [*Sinclair et al.*, 1976; *Mercado et al.*, 2006; *Houborg et al.*, 2009*; Alton et al.*, 2007], overestimate [*de Pury and Farquhar*, 1997; *Dai et al.*, 2004], or underestimate [*Chen et al.*, 1999; *Friend*, 2001; *Mercado et al.*, 2007] eddy covariance (EC) measurements. Our study is the first to systematically investigate big-leaf and two-leaf upscaling strategies for canopy photosynthesis estimation using a well-tested ecosystem model across 11 flux tower sites in North American boreal and temperate regions. Our hypotheses are (1) big-leaf upscaling will underestimate canopy-level GPP compared with the two-leaf upscaling, and this underestimation is strongest in dense forest canopies with large fractions of shaded leaves, and (2) variance in daily GPP explained by the big-leaf approach will be less than that explained by the two-leaf approach when canopies absorb a significant quantity of diffuse radiation. On the basis of the investigation of these hypotheses against carbon flux data, we explain the likely physiological mechanisms that may lead to big-leaf or two-leaf mismatches against observations.

2. Methods

2.1. Study Sites

[11] We selected 11 North American forested eddy covariance flux tower sites that are part of the Ameriflux and Canadian Carbon Program networks and used in the North American Carbon Program (NACP; http://www.nacarbon.org/nacp/) site-model intercomparison interim synthesis. The sites span North America from northern boreal latitudes (lat = 68°) to midlatitudes (lat = 35°). These sites are six broadleaf deciduous forests: the Old Aspen site (CA-Oas; Prince Albert National Park, Saskatchewan, Canada), the University of Michigan Biological Station (U.S.-UMB; Michigan), Sylvania Wilderness Area (U.S.-Syv; Michigan), Missouri Ozark Site (U.S.- MOz; University of Missouri's Baskett Wildlife Research and Education Area, Missouri), the Walker Branch watershed (U.S.-WBW; National Environmental Research Park, Oak Ridge, Tennessee) and the Tonzi ranch (U.S.-Ton; California); three evergreen coniferous forests: the Old Black Spruce forest (CA-Obs; Prince Albert National Park, Saskatchewan, Canada), the main tower of Howland Forest (U.S.-Ho1; Maine), and the Niwot Ridge temperate forest (U.S.-NR1; Roosevelt National Forest in the Rocky Mountains, Colorado); and two sites that could be classified as shrublands: Ivotuk (U.S.-Ivo, Alaska) and Mer Bleue (CA-Mer; Mer Bleue Eastern Peatland, Ontario, Canada).

[12] Strictly speaking, the oak woodland savanna Tonzi ranch is not per se a broadleaf site [*Chen et al.*, 2008]; however, since the overstory vegetation is 40% dominated by blue oak (*Quercus douglasii*), many regional to global ecosystem models classify the site as broadleaf deciduous forest, and, for consistency, we do the same. The same argument could be made for the Mer Bleue peat bog, which is a wetland site that we classify under the shrubland category while aggregating the detailed land-cover types (i.e., GLC2000; see section 2.6) to six plant functional types. Detailed descriptions of these sites are summarized in Table 1.

[13] The observed values of net ecosystem exchange (NEE) were corrected for storage and filtered to remove conditions of low turbulence. The gaps in the observations at all sites were filled using a consistent algorithm based on moving-window regression of NEE to environmental parameters [*Barr et al.*, 2004]. Consistency in gap filling and NEE decomposition into GPP maintains fidelity of comparison across sites [*Desai et al.*, 2008]. Additionally, estimates of uncertainty due to random processes and uncertainty due to the friction velocity filtering were also computed for each site [*Barr et al.*, 2004; *Schwalm et al.*, 2010]. GPP at each tower site was inferred from an established, common algorithm that first estimates ecosystem respiration (ER) by moving-window regression of nighttime NEE to temperature and establishes GPP as the difference between modeled ER and NEE. In this analysis, GPP was aggregated to daily integrals to reduce the impact of random errors.

2.2. Ecosystem Modeling

[14] Simulations of GPP for both two-leaf and big-leaf models were made using the Boreal Ecosystem Productivity Simulator (BEPS) [*Liu et al.*, 1997, 1999, 2002; *Chen et al.*, 1999; *Ju et al.*, 2006]. BEPS is driven by gridded meteorological (incoming shortwave radiation, air temperature, specific humidity, precipitation, and wind speed) and soil water holding capacity [*Liu et al.*, 2002] data sets, and SPOT4 remotely sensed vegetation parameters (land-cover type and leaf area index(LAI)). Although the model was initially developed for boreal ecosystems and intensively tested over the Canadian landmass, it has been successfully implemented in temperate and tropical environments as well by adjusting the inputs to local environmental and biophysical conditions [e.g., *Wang et al.*, 2004; *Zhou et al.*, 2007; *Feng et al.*, 2007].

[15] The model calculates hourly carbon fixation by scaling Farquhar's leaf biochemical model [*Farquhar et al.*, 1980] up to the canopy level following *Chen et al.* [1999]. With spatially explicit input data on vegetation, meteorology, and soil, BEPS can be run either pixel by pixel over a defined domain or can simulate canopy photosynthesis at a particular geographic location. Stomatal conductance is calculated by a modified version of the Ball-Woodrow-Berry model [*Ball et al.*, 1987]. Incoming radiation is separated into diffuse and direct components following the semiempirical approach given by *Erbs et al.* [1982], *Black et al.* [1991], and *Chen et al.* [1999]. The mean energy budgets of sunlit and shaded leaves are calculated using the methods of *Chen et al.* [2007]. Since the emphasis of our study is on the differences between big-leaf and two-leaf approaches in simulating measured GPP for the purpose of demonstrating the issues with leaf internal resistance in the big-leaf formulation, we focus on the model's ability in capturing day-to-day GPP variability in this study. Therefore, the hourly modeled results are aggregated to daily values in order to clearly demonstrate the difference in model's response to day-to-day meteorological variations (particularly radiation) (Figure 2). Key equations of the model are described in Appendix A.

Table 1. The Description of Studied Sites[a]

Site ID and Available Time Frame	IGBP	Location	Elevation (m ASL)	P (mm)	T_{air} (°C)	LAI ($m^2 m^{-2}$)	Clumping Index	Arboreal Composition	Reference
CA-Oas (1997–2006)	DBF	53.78°N, 106.28°W	530	428.53	0.34	3	0.70 ± 0.047	Trembling aspen, Balsam poplar	*Barr et al.* [2004]
U.S.-UMB (1999–2003)	DBF	45.56°N, 84.71°W	234	750	6.2	3.7	0.70 ± 0.047	Trembling aspen and paper birch	*Gough et al.* [2008]
U.S.-Syv (2002–2006)	DBF	46.24°N, 89.35°W	540	826	3.8	4	0.70 ±0.047	Sugar maple, eastern hemlock and yellow birch	*Desai et al.* [2005]
U.S.-MOz (2005–2006)	DBF	38.74°N, 92.2°W	219	940	12.11	4	0.70 ± 0.047	Oak, shagbark hickory, sugar maple, eastern red cedar	*Gu et al.* [2006]
U.S.-WBW (1995–1999)	DBF	35.96°N, 84.29°W	250– 330	1352	14.21	6	0.70 ± 0.047	Oak, hickory, tulip poplar, maple and loblolly pine	*Baldocchi and Wilson* [2001]
U.S.-Ton	DBF	38.43°N; 120.97°W	177	496–616	15.5–16.5	0.6	0.70 ± 0.047	Blue oak and foothill pine	*Xu and Baldocchi* [2003]
CA-Obs (2000–2006)	ENF	53.987°N, 105.118°W	629	406	0.79	4.5	0.74 ± 0.057	Black spruce and tamarack	*Jarvis et al.* [1997]
U.S.-Ho1 (1996–2004)	ENF	45.2°N, 68.7°W	60	1040	6.7	5.3	0.74 ± 0.057	Red spruce, eastern hemlock, balsam fir, white pine and white cedar	*Xiao et al.* [2005]
U.S.-NR1 (1999–2007)	ENF	40.03°N, 105.55°W	2850–3050	800	2	4	0.74 ± 0.057	Subalpine fir, engelmann spruce and lodgepole pine	*Bradford et al.* [2008]
U.S.-Ivo	SHR	68.49°N, 155.75°W	568	150	−12.3	N/A	0.75 ± 0.059	Deciduous shrub, tussock-forming sedge, Spagnum mosses.	*Epstein et al.* [2004]
CA-Mer		45.41°N, 75.52°W	910		5.8	N/A	0.75 ± 0.059	Sphagnum spp., Labrador tea, leatherleaf, blueberry, cotton grass, sedge	*Frolking et al.* [1998]

[a]IGBP, International Geosphere-Biosphere Programme; DBF, deciduous broadleaf forest; ENF, evergreen needle-leaf forest; SHR, open shrubland; P, precipitation; T_{air}, air temperature; LAI, leaf area index; CA-Oas, Old Aspen site (California), U.S.-UMB, the University of Michigan Biological Station (Michigan), U.S.-Syv, Sylvania Wilderness Area (Michigan), U.S.-MOz, Missouri Ozark Site (Missouri), U.S.-WBW, the Walker Branch watershed (Tennessee), CA-Obs, Old Black Spruce forest (Canada); U.S.-Ho1, Howland Forest (Maine), U.S.-NR1, Niwot Ridge forest (Colorado). Clumping index after the work by *Chen et al.* [2005].

2.3. Two-Leaf Approach

[16] BEPS was originally a two-leaf model that calculated GPP separately for sunlit (LAI_{sun}) and shaded (LAI_{sh}) parts of overstory and understory layers following the leaf stratification strategy [*Norman*, 1982]. The total canopy photosynthesis (A) is then estimated as the sum of representative sunlit (A_{sun}) and shaded leaf (A_{sh}) photosynthesis rates:

$$A = A_{sun}\mathrm{LAI}_{sun} + A_{sh}\mathrm{LAI}_{sh}. \quad (1)$$

[17] Both rates of photosynthesis are calculated using Farquhar's leaf biochemical model [*Farquhar et al.*, 1980] combined with a physical model describing the CO_2 flow from inside the stomatal cavity to the free air [*Leuning*, 1997]. We used separate leaf-level biochemical parameters for each canopy stratum, thereby acknowledging physiological differences in maximum carboxylation and electron transport rates that may have consequences for GPP (see Appendix A for equations).

[18] The total leaf area index (LAI) is separated into sunlit and shaded LAI using the original formulation of *Norman* [1982] with consideration of a foliage clumping index proposed by *Chen et al.* [1999]:

$$\mathrm{LAI}_{sun} = 2\cos\theta\left(1 - e^{-G(\theta)\Omega LAI/\cos\theta}\right), \quad (2a)$$

$$\mathrm{LAI}_{sh} = \mathrm{LAI} - \mathrm{LAI}_{sun}, \quad (2b)$$

where θ is the solar zenith angle and $G(\theta)$ is the foliage projection coefficient taken as 0.5 assuming a spherical leaf angle distribution. Ω characterizes the leaf spatial distribution pattern in terms of the degree of its deviation from the random case (being unity for randomly distributed leaves and less than one for clumped canopies) and influences radiation interception by the canopy at a given θ as described by Beer's law.

2.4. Big-Leaf Approach

[19] In Farquhar's model, the leaf-level photosynthetic capacity is described as the sum of all the chloroplast capacities in a given unit area, and the chloroplast properties are assumed to scale with the internal light gradient of the leaf [*Farquhar and von Caemmerer*, 1982]. A similar argument has been applied to plant canopies assuming an optimal distribution of leaf nitrogen through the canopy, which occurs when nitrogen is distributed in proportion to the distribution of the solar irradiance absorbed by the canopy, averaged over the time that leaves are able to acclimate (i.e., several days to a week). This implies that the vertical profile of photosynthetic capacity covaries more or less linearly with leaf nitrogen content [e.g., *Ingestad and Lund*, 1986]. Consequently, if the distribution of photosynthetic capacity among leaves in a canopy is proportional to the profile of absorbed irradiance (described by Beer's law), then the canopy can be treated as a homogeneous entity (i.e., big leaf), and the equations usually applied to single leaves might be used for the entire canopy [*de Pury and Farquhar*, 1997; *Farquhar*, 1989]. Stomatal conductance (g) upscaled to the canopy level by means of the total LAI (i.e., gLAI), electron transport rate is calculated from absorbed canopy-

Table 2. Biochemical Parameters Used in This Study as Compared With Literature-Reported Values[a]

Land- Cover Type	V_m (mmol m^{-2} s^{-1})		χ_n (m^2 g^{-1})	m		g_0	
	Range of Literature Values[b]	Big-Leaf Fitted Value		Range of Literature Values[b]	Big-Leaf Fitted Value	Range of Literature Values[b]	Big-Leaf Fitted Value
Broadleaf	15–100 (57 ± 7)	174	0.59	5–11 (6 ± 1.5)	12	0.011–0.0175 (0.01 ± 0.004)	0.002
Conifer	15–130 (62.5 ± 17)	203	0.33	5–11 (8 ± 3)	10	0.011–0.00175 (0.013 ± 0.004)	0.003
Shrubland	25–90 (58 ± 20)	120	0.57	5–8 (6 ± 1.5)	12	0.011–0.00175 (0.013 ± 0.003)	0.01

[a]Literature-reported values are from *Leuning* [1995], *Medlyn et al.* [1999b], *Jogireddy* [2004], *Baldocchi and Xu* [2005], *Op de Beeck et al.* [2009], *Kattge et al.* [2009], *Chen et al.* [2012]. Note that following the strong linear correlation between V_m and J_{max} reported elsewhere [e.g., *Jogireddy*, 2004], the latter was taken as a constant fraction of the former.
[b]Values in parentheses indicate adopted value ± STD.

level PAR and net photosynthesis in an unshaded leaf (A_0), which is consequently scaled to the total canopy value as proposed by *Sellers et al.* [1992] and described in detail in numerous publications [e.g., *Friend*, 2001; *Arora*, 2003; *Mercado et al.*, 2006, 2007; *Alton et al.*, 2007]:

$$A = A_0 f_{\text{scale}}, \tag{3}$$

where the multiplicative factor (f_{scale}) is equal to (1-exp(-k*LAI))/k and k is the canopy PAR extinction coefficient.

2.5. Clumping Simulations

[20] Foliage clumping increases the probability of leaf overlapping and, as a result, decreases the probability of a leaf exposure to the direct radiation. A decrease in Ω (increasing clumping) results in a decrease of LAI_{sun} and a consequent increase in the fraction of the shaded leaves. Since shaded leaves typically have higher light-use efficiency (photosynthetic performance per unit incident photon flux density), then for extremely clumped canopies such as coniferous forests ($0.5 < \Omega < 0.7$) [*Chen et al.*, 1997], LAI_{sh} should contribute significantly to total canopy productivity. Furthermore, since Ω influences the ratio between sunlit and shaded leaves (as in the two-leaf case) or changes in PAR-intercepted area (as in the big-leaf case), it should have a considerable effect on canopy-level GPP [*Baldocchi and Harley*, 1995; *Chen et al.*, 2003, 2012]. Typical values of Ω are 0.5–0.7 for conifer forests, 0.7–0.9 for broadleaf forests, and 0.9–1.0 for grass and crops [*Chen*, 1996; *Chen et al.*, 1997].

[21] After evaluations of two-leaf and big-leaf models against tower flux measurements, the effect of foliage clumping on GPP estimation was systematically investigated through a sensitivity analysis with the value of clumping index as an input in equation (2a) varying in a large range from 0.3 (very clumped) to 1 (randomly distributed foliage elements). This sensitivity analysis allows us to demonstrate the contribution of shaded leaves to canopy-level GPP and the sensitivity of this contribution to clumping. Both points can then be used to support or refute the necessity of sunlit-shaded leaf separation for modeling canopy photosynthesis.

2.6. Model Parameterization and Forcing

[22] Since our main objective is to compare performances of two strategies of leaf-to-canopy upscaling using regional to global ecosystem models, where site-specific tuning is not preferred, leaf photosynthetic parameters such as maximum carboxylation rate ($V_{c,max}$), electron transport rate (J_{max}) (equations (A2a) and (A2b), respectively), residual conductance (g_0), and the slope of A to g relationship (in meters) were kept the same for both two-leaf and big-leaf models. Thus, the differences between the results can be solely explained by the mathematical formulation of these models. Our approach is justified because adjustment or aggregation of leaf parameters through the canopy, as has been proposed [e.g., *Rastetter et al.*, 1992], is physiologically unrealistic for productivity modeling with big-leaf models (as will be shown further in this paper) and will turn big-leaf into a two-leaf or multilayered model (since it is impossible to obtain canopy-level parameters without an accurate canopy-level model), defeating the very purpose of big-leaf modeling.

[23] Although a wide variety of the values of leaf biochemical parameters is well presented in the current literature [*Wullschleger*, 1993; *Leuning*, 1995; *Medlyn, et al.*, 1999a; *Wolf et al.*, 2006; *Kattge et al.*, 2009; *Chen et al.*, 2012], there is still large uncertainty regarding their exact values classified per species or plant functional types (PFTs) [*Bonan*, 1995; *Kattge et al.*, 2009]. The range of the reported values for different kinds of land-cover classifications is well summarized elsewhere [*Wullschleger*, 1993; *Medlyn et al.*, 1999b; *Jogireddy*, 2004; *Baldocchi and Xu*, 2005; *Chen et al.*, 2012] and presented here in Table 2.

[24] Because BEPS, as well as other land-surface models, aims at regional applications with remote sensing inputs, our analysis used biochemical parameters derived for different plant functional types (PFTs) distributed among distinct climate zones. Thus, as mentioned by *Groenendijk et al.* [2010], running it globally requires the parameters to be provided for every model grid cell, which is typically done by setting unique value for each PFT. For this reason we adopted leaf-level values for different PFTs from *Kattge et al.* [2009], who conducted metadata analysis with 723 data points (Table 2, values in parentheses). However, accounting for the fact that the values of these parameters could be different at a latitudinal perspective, they have been adjusted with respect to climatic region (i.e., latitude). The reported value of standard deviation (Table 2) provides us with such flexibility. Nonetheless, one should bear in mind that latitude-based parameterization does not look very practical from a remote sensing point of view since the boundary of climate regions could not be easily defined.

[25] BEPS was initialized to run for different land covers or a mixture of land covers, including broadleaf forest, coniferous forest, shrublands, C4 plants, and others (mostly crops and grass) aggregated from the detailed 1 km GLC2000 (http://www.eogeo.org/GLC2000) land-cover map, which was derived from SPOT4 VEGETATION imagery.

[26] Daily LAI values at each site were extracted from the global LAI product [*Deng et al.*, 2006], which is based on a

10-day synthesis of SPOT4 VEGETATION images (1 km spatial resolution). The LAI algorithm was developed based on the four-scale geometrical optical model and accounts for the variations of the reflectance in the various bands with the angles of the Sun and the satellite [*Chen and Leblanc*, 1997]. The resulted values are corrected for the clumping based on the global clumping index map produced from the multiangle observations of POLDER 1, 2, and 3 sensors [*Chen et al.*, 2005].

[27] Relevant meteorological inputs to the model included incoming radiation (W m^{-2}), air temperature (°C), specific humidity (g kg^{-1}), precipitation (mm), and a wind speed (m s^{-1}) at 1/2 h resolution. Soil texture for each location was determined based on the fractions of clay, silt, and sand in soil and was used to calculate water holding capacity and soil water scaling parameter [*Ju et al.*, 2006].

[28] For the evaluation of these models, we relied on the canopy-scale measurements of the CO_2 flux made using the eddy correlation technique [*Baldocchi*, 2003]. Site-level meteorological and soil data are also available from Ameriflux and Fluxnet Canada databases. Meteorological data were gap filled following a standard protocol as part of the North American Carbon Program (NACP) synthesis activity. Missing values (i.e., gaps) in the meteorological data records were filled using data of the nearest available climate station in the National Climatic Data Center's Global Surface Summary of the Day database or using DAYMET [*Thornton et al.*, 1997].

3. Results and Discussion

3.1. Magnitude of GPP and Comparisons With Measured Results

[29] Large differences were apparent between two-leaf and big-leaf model estimates of GPP for all sites examined (Figure 1). Since the behavior of both types of simulations is very consistent from year to year, for clarity only one representative year is displayed for each site.

[30] Consistent with our hypothesis, the big-leaf model underestimated measured GPP for all structurally complex ecosystems, as evidenced by slopes < 1. Surprisingly, this underestimation occurred even in shrubland or low-LAI sites. In contrast, the two-leaf model had a slope closer to 1 at all sites, indicating greater fidelity between simulated and tower-derived GPP estimates. With respect to our second hypothesis, the results show that a greater percentage of variability in daily GPP was simulated by the two-leaf than the big-leaf model, especially at structurally complex coniferous sites. These points are primarily supported by the differences in the slope of the relationships between measured and modeled results, i.e., closer to 1 for the two-leaf model (ranging between 0.76 and 0.98, with an average of 0.86 $\pm$ 0.07) and very low for the big-leaf model (ranging from 0.4 to 0.52, with an average of 0.46 $\pm$ 0.04) as well as by coefficient of variation (CV) that equal 1.12, 0.68, and 0.51 for broadleaf, 0.65, 0.85, and 0.57 for conifers, and 1.21, 1.27, and 1.24 for shrublands for measured, two-leaf, and big-leaf models, respectively.

[31] The close similarity between CV for two-leaf and big-leaf for shrubland sites could be explained by the naturally uniform distribution of canopy elements at the wetland site (classified as shrubland). These results support our hypothesis that GPP by structurally complex canopies cannot be adequately simulated by the big-leaf model.

3.2. Physiological Mechanisms of Big-Leaf GPP Underestimation

[32] In contrast to evapotranspiration modeling, for which big-leaf approximation has been considered to be adequate [e.g., *Raupach and Finnigan*, 1988], the underestimation of GPP by the big-leaf model (when given the same leaf parameters as those in the two-leaf model) may be caused in part by simplified assumptions concerning the stomatal regulation of CO_2 exchange as implied in the big-leaf formulation. Since significant resistance to carbon diffusion comes from leaf internal tissues [*Chen et al.*, 1999; *Warren*, 2008], the big-leaf formulation essentially interrupts the pathway of CO_2 flow from the outer air (stomatal cavity) to chloroplasts. By scaling only the stomatal conductance to the canopy level, the big-leaf approach artificially accumulates a large amount of stomata on one theoretical leaf (i.e., stomatal resistances of individual leaves are in parallel to the canopy resistance) while maintaining one leaf internal resistance to the gas flow. In this way, the total resistance to the CO_2 flow is amplified as compared to the realistic case when leaves are all operating in parallel. When multiple layers of leaves work simultaneously, multiple internal resistances would operate in parallel, allowing CO_2 flow to meet less resistance on its pathway from stomatal cavity to photosynthetic site.

[33] Consequently, as was suggested by *Chen et al.* [1999] and presented by *Mercado et al.* [2007], big-leaf performance will be significantly improved by adjusting the vertical distribution of the parameters responsible for the internal control (i.e., V_m, J_{max}, or compensation point). This last point actually signifies that the underestimation of GPP by the big-leaf model is by itself not ultimate proof of the fundamental failure of the big-leaf upscaling strategy, because at local scales, big-leaf underestimation could simply be remedied by parameterization of key model parameters to match observations. Our findings, however, show that consistently low GPP estimates by the big-leaf model for a range of ecosystems pose challenges for regional and global simulations in which these site-specific parameter adjustments are not practical. In this case, the adjusted big-leaf parameters could be (and were in our case) nearly twice as large as published values for a broad array of ecosystem types (Table 2). This outcome is similar to those reported by *Mercado et al.* [2006], who showed increments of more than 60% in order to force big-leaf to match tower measurements.

3.3. Variability of Daily GPP

[34] Even if big-leaf estimates could be boosted by inflating the leaf-level parameters to match observed GPP magnitudes, we have shown that daily and seasonal variability in GPP is more accurately captured by a two-leaf model, further demonstrating the shortcomings of the big-leaf mathematical formulation for GPP modeling. Figure 2 shows day-to-day variations of GPP obtained by the eddy covariance system versus the big-leaf and two-leaf model results, clearly indicating a greater dissimilarity in the amplitude of oscillation on both day-to-day and annual scales for the big-leaf model. Statistically, that dissimilarity was evaluated by comparing two standard measures of dispersion usually used for quantitative expression of the degree of

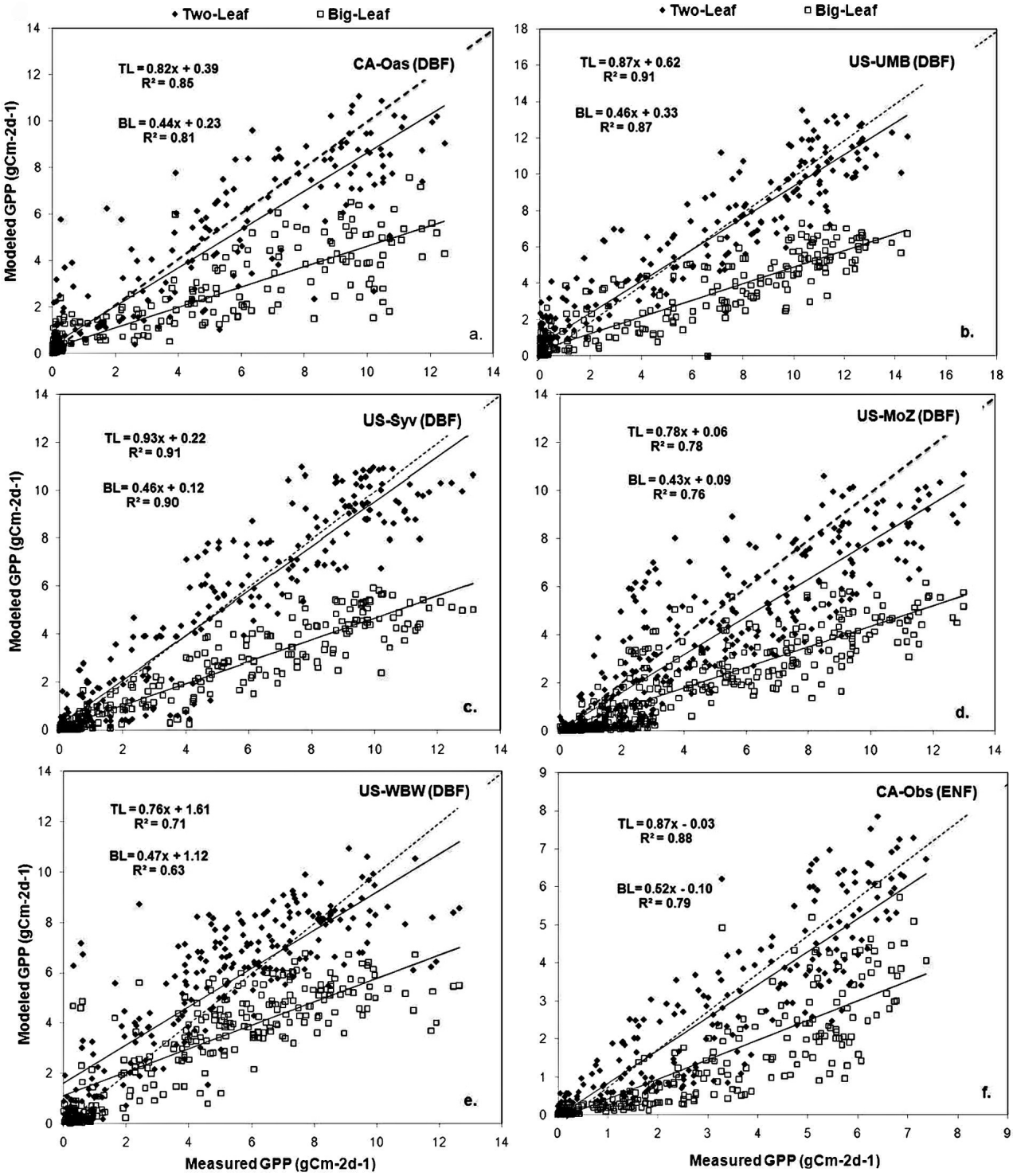

Figure 1. Comparisons of the measured gross primary production (GPP) and the GPP simulated by both two-leaf and big-leaf approaches. (a–e, k) Cases are for deciduous broadleaf forests (DBF in the upper right-hand corner of each subplot). (f–h) Cases are for evergreen needle-leaf forests (ENF in the upper right-hand corner of each subplot). (i, j) Cases are for wetland (capital "WET" at the upper right corner of the subplot) and tundra ("Tun" at the upper right corner of the subplot) sites, respectively. Note that only one representative year is displayed for each site.

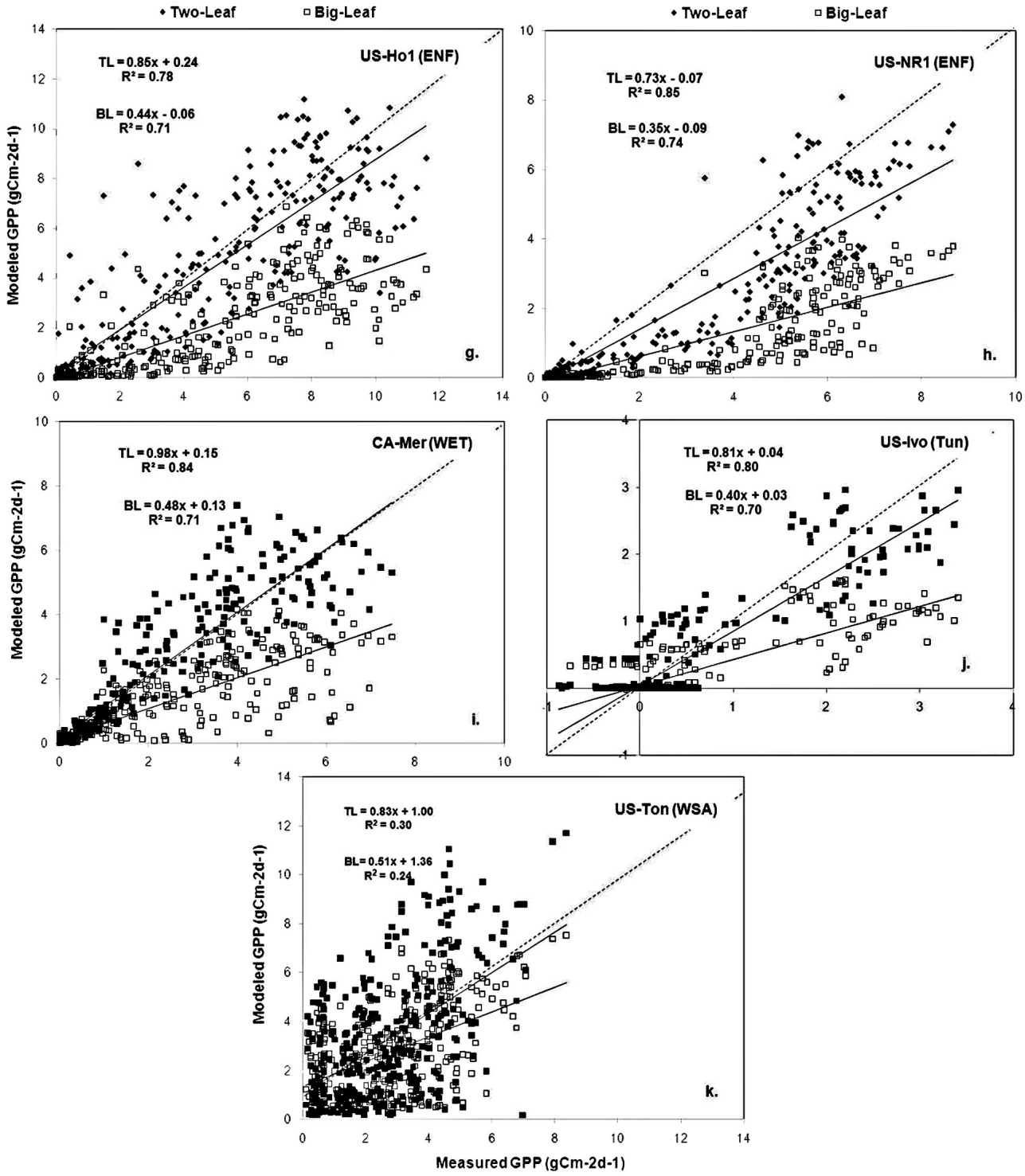

Figure 1. (continued)

variation in population: variance and interquartile range (IQR).

[35] Both measures of variability are much smaller for big-leaf as compared with two-leaf and EC cases (Table 3). Averages values for EC, two-leaf, and big-leaf are 5.8 ± 3.7, 5.2 ± 3, and 1.9 ± 0.9, respectively, for variance, and 7.4 ± 5.3, 6.6 ± 4.0, and 2.6 ± 1.3, respectively, for IQR. Differences in the variances of daily GPP among modeled and measured estimates can be explained by the assumption in the big-leaf model that the entire canopy is a single unshaded leaf located at the canopy top. This approach diminishes the radiation control of, and consequently variation in, CO_2 fixation because even if the radiation is mostly diffuse, irradiance levels often approach light-saturating

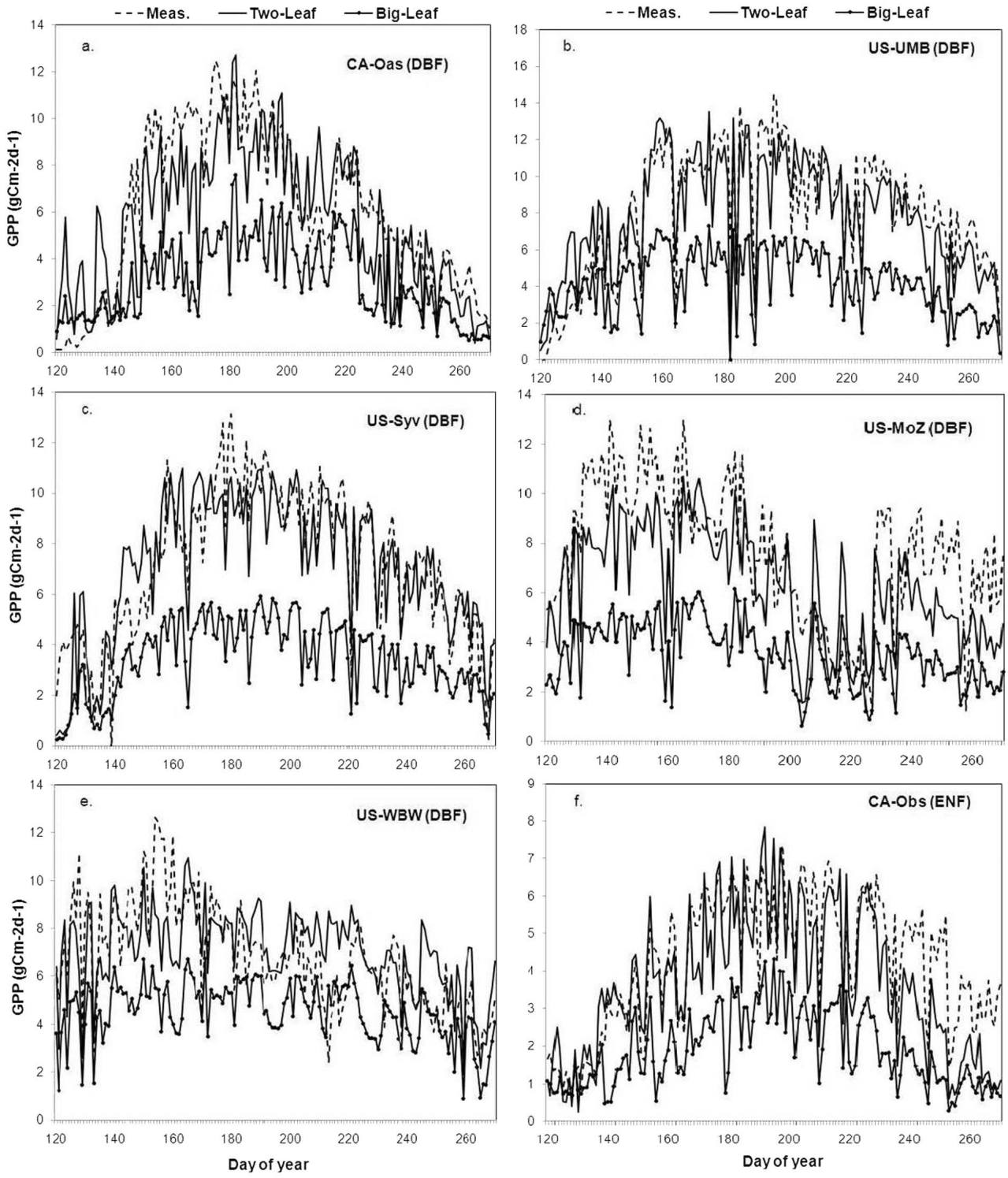

Figure 2. Day-to-day variations of GPPs obtained by the eddy covariance system in comparison with two model simulations.

conditions for a single horizontal leaf and the photosynthesis rate of the big-leaf is mostly determined by the maximum carboxylation rate, which depends on leaf temperature and nutrient status. This representation leads to the inability of the big-leaf approach to differentiate between clear and overcast days, resulting in unrealistic loss of model sensitivity to radiation load, and attenuates day-to-day amplitude in modeled GPP. The same lack of sensitivity explains the generally flat seasonal variation (Figure 2). In contract, the two-leaf model is sensitive to radiation variation because shaded leaves are often limited by the electron transport rate determined by the incident radiation level rather than by

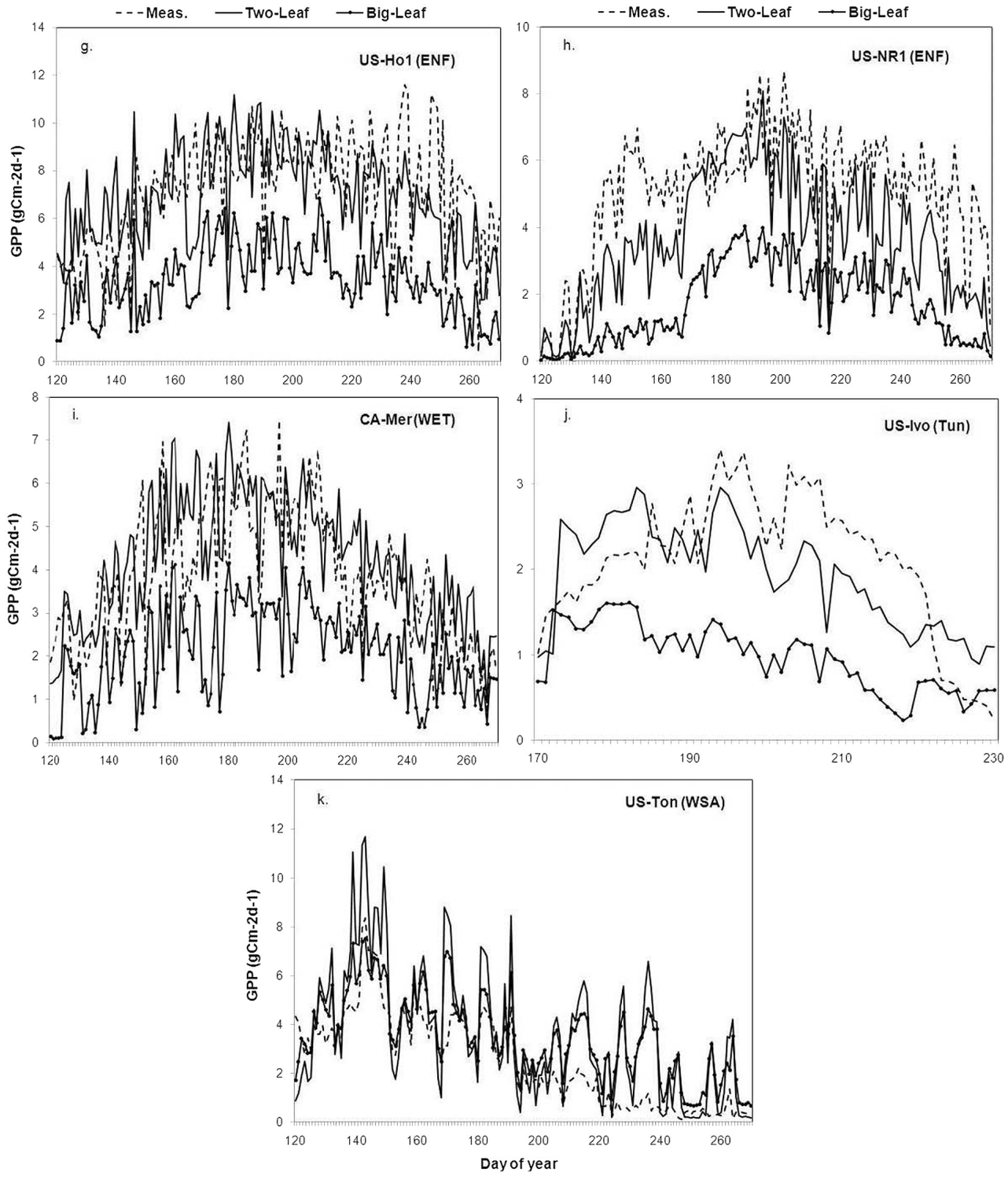

Figure 2. (continued)

the maximum carboxylation rate. Under low-radiation conditions, canopy-level photosynthesis simulated by the two-leaf model is therefore strongly sensitive to small changes in incident radiation.

[36] Although the adjustment of the input parameters can improve the ability of a big-leaf model to reproduce the seasonal trend of simulated GPP as presented in Figure 3 for two selected sites, the lack of variance reproduced is still pronounced on a day-to-day scale compared with the two-leaf model results, as the variance of the simulated distribution remains below the observed case. *Mercado et al.* [2006] obtained similar results regarding the dispersion of

Table 3. Measures of Dispersion for Day-to-Day Variations of GPP Obtained by the Eddy Covariance, EC, Measurements and Simulated by Two-Leaf and Big-Leaf Models[a]

	Variance[b]				Interquartile Range[c]		
			Big-Leaf				
Site	EC Value	Two-Leaf Value	Value	Fitted Value	EC Value	Two-Leaf Value	Big-Leaf Value
Oas: 54° (DBF)	11.8	9.3	2.9	4.1	17.8	13.1	3.7
Syv: 46° (DBF)	8.5	7.9	2.2	3.2	8.6	9.2	3.1
UMB: 46° (DBF)	12.2	10.0	3.0	4.9	15.0	12.4	4.3
MOz: 39° (DBF)	7.5	5.2	1.7	3.2	11.1	6.7	2.3
WBW:35° (DBF)	4.8	2.9	1.5	3.1	6.2	2.1	1.4
Ton: 38° (WSA)	3.6	7.0	2.9	n/a	3.5	9.3	4.3
Obs: 54° (ENF)	3.1	3.6	2.0	2.4	3.9	5.7	2.7
Ho1: 45° (ENF)	5.1	4.1	2.1	4.8	6.9	5.4	3.4
NR1: 40° (ENF)	3.7	3.7	1.3	2.6	3.6	5.4	1.8
Mer: 45° (WET)	2.4	2.2	1.1	2.0	3.4	2.9	1.4
Ivo: 68° (TUN)	1.3	0.9	0.3	1.8	1.2	0.7	0.2
AVG	5.8	5.2	1.9	3.2	7.4	6.6	2.6
STD	3.7	3.0	0.9	1.1	5.3	4.0	1.3
Average (±STD) for DBF	8.04 ± 3.1	7.04 ± 2.96	2.37 ± 0.68	3.72 ± 0.79	10.36 ± 4.72	8.79 ± 4.5	3.19 ± 1.14
Average (±STD) for ENF	3.94 ± 1.01	3.79 ± 0.25	1.82 ± 0.41	3.25 ± 1.3	4.79 ± 1.8	5.5 ± 0.19	2.62 ± 0.81
Average (±STD) for SHR	1.85 ± 0.72	1.53 ± 0.88	0.66 ± 0.57	1.89 ± 0.19	2.28 ± 1.54	1.8 ± 1.61	0.8 ± 0.85

[a]Letters in parentheses indicate deciduous broadleaf forests (DBFs), evergreen needle-leaf forests (ENFs), woody savanna (WSA), wetland (WET), or tundra (TUN) sites; AVG, average; STD, standard deviation. Fitted value stands for the case in which photosynthetic parameters have been arbitrarily increased in the big-leaf simulations to match the values measured by EC.

[b]$Variance = \frac{1}{n}\sum_{i=1}^{n}(x_i - \bar{X})^2$, where x_i is a measured value, X is an average for the growing season, and n is the number of observations.

[c]Interquartile Range = CDF^{-1} (0.75) − CDF^{-1} (0.25), where CDF is a cumulative distribution function.

simulated data for an Amazonian forest, showing simulated GPP tightly distributed around an average and failing to capture the variability measured by an eddy covariance system. This lack of day-to-day variability in GPP simulated by the big-leaf model is caused not only by its inability to reflect the radiation control on shaded leaf photosynthesis as analyzed above but also by the amplified leaf internal resistance to the CO_2 flow. The big-leaf formulation reduces only the stomatal resistance for multiple layers of leaves while the leaf internal resistance is unchanged no matter how many layers of leaves are operating simultaneously (i.e., internal resistances are in parallel in reality). This amplified internal resistance in the big-leaf formulation makes the model insensitive to driving factors affecting the canopy photosynthesis.

3.4. Impact of Canopy Clumping on Photosynthesis Upscaling

[37] Our results indicate that discrepancy between the EC-measured and big-leaf modeled results is larger for coniferous than deciduous and shrubland sites because canopy structural features constrain GPP. This large discrepancy among land-cover types demonstrates the importance of the shaded part of a canopy for general evaluation of GPP, especially in clumped canopies, which are common for coniferous forests. Consequently, it is likely that the basis of the disagreement of measured (and two-leaf) versus big-leaf derived estimates of GPP is related to canopy structure and that this disagreement will exacerbate with increased clumping (i.e., a decrease in clumping index), as is the case for conifer sites. This suggestion is supported by the relative error (RE) between measured and big-leaf-simulated GPP estimates: ($RE = \frac{|\text{measured}-\text{bigleaf}|}{\text{measured}}$ were ∼29% higher for coniferous (61%) than for broadleaf (32%) and shrubland (47%) stands). In contrast, the difference between measured and two-leaf modeled GPPs for these land-cover types was only ∼4%.

[38] The direct effect of changes in canopy architecture on simulated productivity for all sites is shown in Figure 4 by portraying the relative difference between two-leaf and big-leaf GPPs against the clumping index, which demonstrates that discrepancies between two-leaf and big-leaf estimates of GPP grew as clumping increases (decreasing clumping index). This trend can be explained by the contribution of the shaded part of the canopy to the total GPP because, theoretically, any decrease in Ω implies a decrease of LAI_{sun} and a consequent increase of LAI_{sh}. Even though a shaded leaf receives much less radiation than a sunlit one and its total quantum yield and stomatal conductance typically do not exceed those of a sunlit leaf [*Šprtová and Marek*, 1999], shaded leaves generally display greater light sensitivity at lower irradiances (i.e., higher light-use efficiency) and thus may constitute a large fraction of total canopy photosynthesis under conductions of high diffuse light [*Alton*, 2008; *Gu et al.*, 2002]. The contribution of LAI_{sh} to the total canopy photosynthesis can be as high as 40%–60% [*Mercado et al.*, 2006].

[39] Since a big-leaf model does not partition the canopy, an increase in clumping merely leads to a decrease in overall LAI (LAI_{tot}) and a resulting decrease in total simulated GPP. Consequently, the difference between two-leaf and big-leaf simulated GPPs rises to its highest for most clumped canopies. In the case of low clumping, the contribution of LAI_{sh} will be much lower than that of LAI_{sun}, and the differences between two-leaf and big-leaf estimates of GPP become smaller. However, even for Ω close to unity, big-leaf simulated GPP was only ∼50% of that obtained by two-leaf approach, suggesting that the contribution of LAI_{sh} should not be ignored in any case.

[40] Also apparent are differences in the ratio of big-leaf to two-leaf GPPs between the boreal (or cold) forest sites (CA-Oas, CA-Obs, and U.S.-NR1) and the sites located at lower latitudes. These differences are pronounced

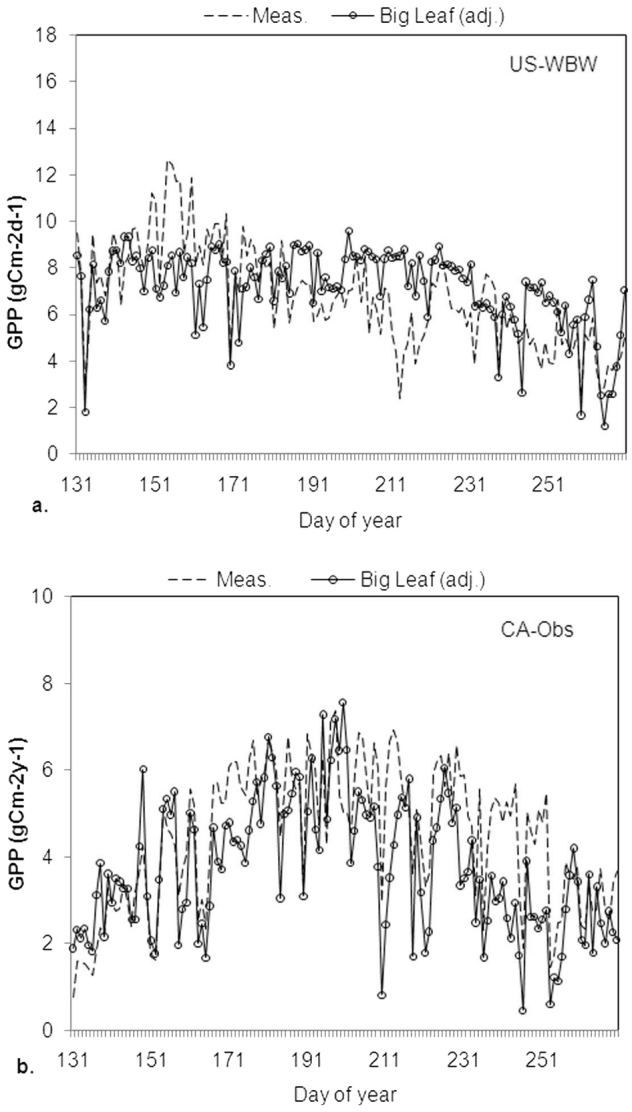

Figure 3. Day-to-day variations of GPPs simulated by the adjusted (adj.) big-leaf model in comparison with a measured case. See Table 2 for adjusted parameters.

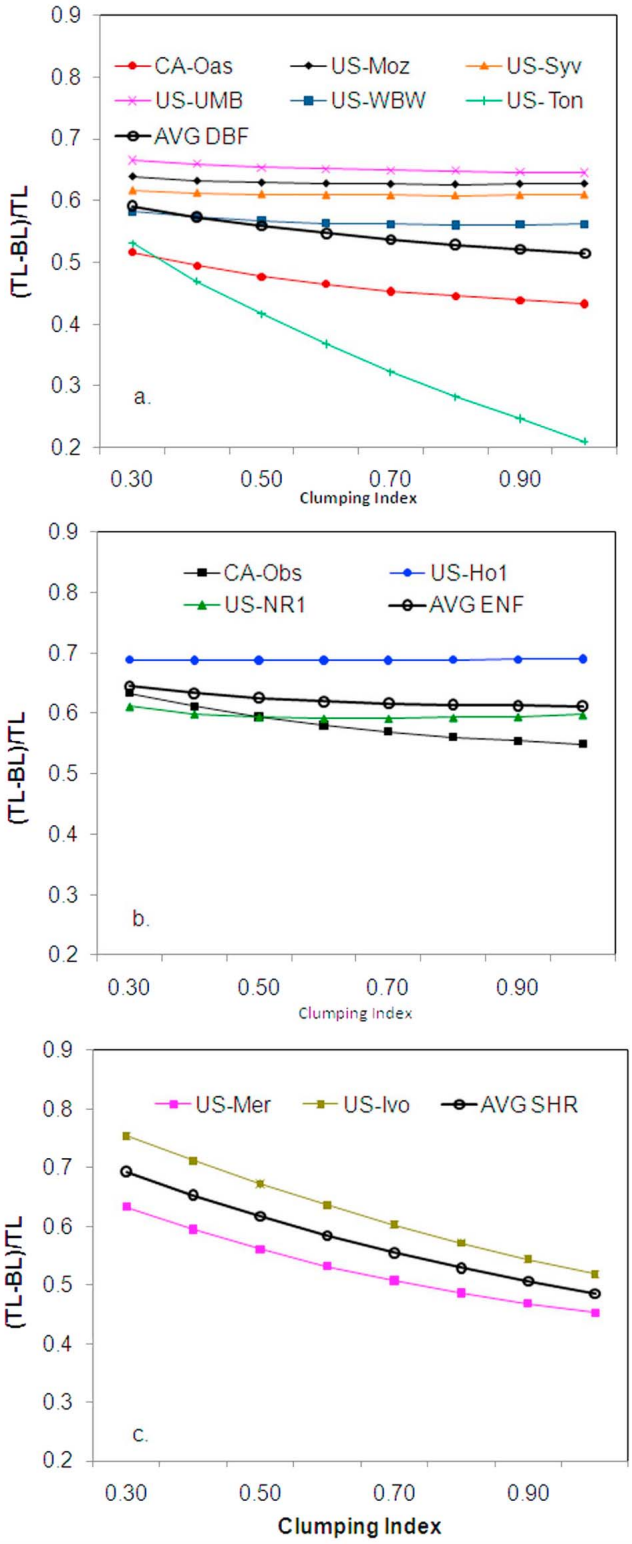

Figure 4. Relative differences between GPP simulated by two-leaf (TL) and big-leaf (BL) models versus various clumping index (i.e., the ratio between sunlit and shaded leaves) for (a) deciduous broadleaf forests (DBFs), (b) evergreen needle-leaf forests (ENFs), and (c) shrubland (SHR) sites.

regardless of Ω and could be explained by the fact that even though plants enhance their light-use efficiency under low irradiance, this increase cannot compensate for the general decrease in canopy productivity under predominantly low-radiation loads in high-latitude cold environments. LAI_{sh} in such environments is much less active than in warmer climates, and its contribution to a total photosynthesis is ~10% lower, even for extremely clumped cases. In warmer environments the contribution of LAI_{sh} remains stable over the entire range of clumping. In colder climates, its behavior was more similar to that of a deciduous forest.

[41] An outlier in our results is the semiarid savanna site (U.S.-Ton), for which both models do not perform well in simulating its GPP. We suggest that the reason for such a similarity lies in low water availability and low light-use efficiency under predominantly high direct radiation loads, causing low stomatal conductance, which is not well captured

by both models. This point, however, requires further investigation to properly scale between photosynthesis and stomatal conductance using the Ball-Woodrow-Berry equation.

3.5. Canopy Architecture and Global Scale GPP Modeling

[42] Our finding that foliage clumping affects the outcome of carbon exchange simulations for a broad array of ecosystems when the canopy is treated as a big leaf indicates that poor representation of canopy architecture in models could have a dramatic impact on global estimates of GPP. This point is especially critical when using global LAI maps derived from optical remote sensing observations that usually relate more closely to the effective LAI rather than the true LAI [*Chen et al.*, 2002]. Because LAI maps provide a basic input for many ecosystem models, incorrect representation of the ratio of sunlit-to-shaded leaf fractions in a canopy imbedded in effective LAI could lead to significant errors in modeled GPP on the global scale.

[43] *Chen et al.* [2012] investigated the impact of foliage clumping on the global GPP estimation by modeling productivity for different treatments of the canopy architecture using the effective and true LAI values. Their results indicate that for accurate global terrestrial GPP estimation, vegetation structure needs to be carefully described, at least in terms of precise representation of the ratio between shaded and sunlit parts. Inaccuracies in such a representation lead to either overestimation by about 8% ($\sim$11 $\pm$ 1.6 picograms of carbon (pgC)) when the true LAI is used without considering clumping (sunlit LAI is overestimated and shaded LAI is underestimated) or underestimation by 15% ($\sim$20.5 $\pm$ 3 pgC) when the effective LAI is used without considering clumping (sunlit LAI is accurate but shaded LAI is underestimated). Their study found that shaded leaves contribute 56%, 40%, and 39% to the total GPP for broadleaf evergreen forest, evergreen conifer forest, and shrub vegetation, respectively, with a global average of this ratio of 39%. Such a pronounced contribution cannot be ignored and has to be taken into account while upscaling from leaf to canopy in modeling vegetation photosynthesis, regardless of the upscaling approaches used.

4. Conclusions

[44] By comparing the two most common strategies of leaf-to-canopy upscaling of CO_2 fixation in ecosystem models across three land-cover types of varying canopy structural complexity in North America, we demonstrated that the separation of the canopy into its shaded and sunlit parts substantially improves the accuracy of modeled gross primary productivity magnitude and daily variability. Our multisite intercomparison adds evidence that big-leaf photosynthesis models should be discouraged or significantly modified for use in regional ecosystem modeling of GPP and demonstrates that a two-leaf approach is superior to the big-leaf one. Underestimation of GPP together with lower sensitivity of GPP to irradiance under the big-leaf mathematical formulation may be explained by (1) unrealistic amplification of leaf internal control on CO_2 pathway from stomatal cavity to photosynthetic machinery, and (2) inaccurate representation of variability in direct or diffuse radiation and its effect on CO_2 fixation.

[45] Our study demonstrates that separating a canopy into sunlit and shaded leaf components (i.e., the two-leaf approach) markedly outperforms the big-leaf approach in simulating GPP for a wide range of ecosystem types with different complexity of canopy architecture. Among the coniferous, deciduous, and shrubland ecosystems examined, the difference between big-leaf and two-leaf models was most pronounced for coniferous sites, which display the highest canopy clumping. Under a given sky condition, clumped canopies have more shaded leaves than those that are less clumped, and therefore GPP is more underestimated by the big-leaf model when considering structurally complex canopies because of its inability to consider the contribution of shaded leaves. Our foliage clumping sensitivity analysis showed that for extremely clumped canopies, the contribution of the shaded part to the total simulated GPP can be as high as 70% and never below $\sim$40%, even for randomly oriented leaves. These results indicate that accurate estimation of GPP for a broad array of canopy architectures requires quantitative understanding of the leaf area arrangement within the canopy and highlights the value of the two-leaf upscaling strategy.

Appendix A

A1. Canopy Photosynthesis

[46] The rates of photosynthesis are calculated by combining Farquhar's model [*Farquhar et al.*, 1980] with a model describing the flow of CO_2 from inside the stomatal cavity to the free air [*Leuning*, 1997]:

$$A_c = \frac{1}{2}\left\{(C_a+K)g + V_m - R_d - \sqrt{[(C_a+K)g + V_m - R_d]^2 - 4[V_m(C_a-\Gamma) - (C_a+K)R_d]g}\right\}, \tag{A1a}$$

$$A_j = \frac{1}{2}\left\{(C_a+2.3\Gamma)g + 0.2J - R_d - \sqrt{[(C_a+2.3\Gamma)g + 0.2J - R_d]^2 - 4[0.2J(C_a-\Gamma) - (C_a+0.2J)R_d]g}\right\}, \tag{A1b}$$

where A_c and A_j are Rubisco-limited and light-limited gross photosynthesis rates, respectively (μmol m^{-2} s^{-1}); V_m is the maximum carboxylation rate (μmol m^{-2} s^{-1}); J is the electron transport rate (μmol m^{-2} s^{-1}); C_i and O_i are the intercellular CO_2 and oxygen concentrations, respectively (mol mol^{-1}); Γ is the CO_2 compensation point without dark respiration (mol mol^{-1}); and K is the function of enzyme kinetics, calculated as $K = K_c(1+O_2)/K_o$ where K_c and K_o are Michaelis-Menten constants for CO_2 and O_2, respectively and could be

found in the work of *Chen et al.* [1999]. The values of the biochemical parameters have been calculated based on the vertical profile of nitrogen content as explained in detail further in this appendix.

[47] The net rate of CO_2 assimilation (either sunlit or shaded parts) is then calculated as

$$A = \min(A_c, A_j) - R_d, \tag{A2}$$

with $R_d = 0.015V_m$ representing a leaf dark respiration.

A2. Stomatal Conductance

[48] The indirect influence of solar irradiance on stomatal conductance (g) becomes apparent in the Ball-Woodrow-Barry equation [*Ball et al.*, 1987] that linearly relates g to the photosynthesis rate (A):

$$g = m\frac{AR_h}{C_s}P + g_0, \tag{A3}$$

where m is a slope that is plant species dependent, R_h is the relative humidity at the leaf surface, P is the atmospheric pressure, C_s is the CO_2 concentration at the leaf surface, and g_0 is a residual conductance.

[49] The influence of soil water content on stomatal conductance is evaluated by adding a soil moisture scaling factor to the Ball-Woodrow-Berry formulation as described in detail by *Ju et al.* [2006]. For simultaneous estimations of A (required for calculation of g; equation (A3)) and g (required for calculation of A; equation (A1)), BEPS uses an iteration procedure exploiting the analytical solution proposed by *Baldocchi* [1994].

A3. Sunlit and Shaded Leaf Irradiance

[50] Total solar radiation above the plant canopy is partitioned into diffuse (I_{dif}) and direct (I_{dir}) components, with the latter a reminder of a former ($I_{\mathrm{dir}} = I_g - I_{\mathrm{dif}}$) [*Erbs et al.*, 1982], which was modified and validated by *Black et al.* [1991] for midlatitudes:

$$\frac{I_{dif}}{I_g} = \begin{cases} 0.943 + 0.734R - 4.9R^2 + 1.796R^3 + 2.058R^4, & R < 0.8 \\ 0.13, & R > 0.8 \end{cases}, \tag{A4}$$

where I_g is the global radiation (W m^{-2}) and $R = [I_g/(S_0 \cos\bar{\theta})]$, with solar constant S_0 = 1367 (W m^{-2}).

[51] The diffuse radiation fraction estimated from this equation is within the variation range of data assembled by *Spitters* [1986] from nine locations around the globe, but is about 5%–10% lower than the mean value across the entire R range. It is important to mention, however, that this equation would underestimate the diffuse fraction for air masses with large aerosol contents.

[52] The sunlit leaf irradiance (I_{sun}) is then calculated as

$$I_{\mathrm{sun}} = \frac{I_{\mathrm{dir}}\cos\alpha}{\cos\theta} + I_{\mathrm{sh}}, \tag{A5}$$

where $\alpha \sim 60°$ is mean leaf-Sun angle for a canopy with spherical leaf angle distribution. The first term on the right-hand side of equation (A5) represents the contribution of the direct beam, while the second term accounts for the diffused radiation (i.e., the mean shaded leaf irradiance), and it is developed based on radiative transfer physics [*Chen et al.*, 1999]:

$$I_{\mathrm{sh}} = \frac{(I_{\mathrm{dif}} - I_{\mathrm{dif,BC}})}{\mathrm{LAI}} + C, \tag{A6}$$

where the first term on the right-hand side quantifies the average diffuse irradiance on shaded leaves (which originates from both the sky irradiance and multiple scattering of the incoming radiation within the canopy) by distributing the total intercepted diffuse radiation from the sky to the total LAI involved; $I_{dif,BC} = I_{dif}e^{(-0.5\Omega LAI/\cos\bar{\theta})}$ is the diffuse radiation below the plant canopy; $\cos\bar{\theta} = 0.537 + 0.025\,\mathrm{LAI}$ is a representative zenith angle for diffuse radiation transmission; and $C = 0.07\Omega I_{dir}(1.1 - 0.1\,\mathrm{LAI})\exp(-\cos\theta)$ is added to include the enhancement of diffuse radiation that is due to multiple scattering of the incoming direct radiation.

A4. Nitrogen-Weighted V_m and J_m for Sunlit and Shaded Leaves

[53] As leaf nitrogen content per unit leaf area N (LAI) decreases exponentially from the top to the bottom of a canopy, it can be expressed as

$$N(\mathrm{LAI}) = N_0\exp(-k_n\,\mathrm{LAI}), \tag{A7}$$

where N_0 is the nitrogen content at the top of the canopy and k_n is the leaf nitrogen content decay rate with increasing depth into the canopy, taken as equal to 0.3, after *de Pury and Farquhar* [1997].

[54] The leaf maximum Rubisco capacity (V_m) is linearly related to leaf nitrogen content (N_l) [*Field*, 1983], that is, $V_m = \chi_n N_l$, in which χ_n is the ratio of measured Rubisco capacity to leaf nitrogen [*de Pury and Farquhar*, 1997; *Dai et al.*, 2004]. Therefore, the vertical profile of leaf nitrogen is modeled as a function of LAI and hence V_m is given by

$$V_m(\mathrm{LAI}) = V_{m,0}\chi_n N(\mathrm{LAI}), \tag{A8}$$

where $V_{m,0}$ is V_m at the top of the canopy (LAI = 0) at 25°C. The values at the top of the canopy (i.e., $V_{m,0}$ and N_0) are taken as their mean values plus one standard deviation. See Table 2 for PFT-dependent values of χ_n.

[55] Because the fractions of sunlit ($f_{\mathrm{sun}} = e^{-\mathrm{kLAI}}$) and shaded ($f_{\mathrm{sh}} = 1\text{-}e^{-\mathrm{kLAI}}$) leaf areas also vary with the depth into the canopy, the mean values of eaf nitrogen content for sunlit and shaded leaves and their corresponding V_m values can be obtained through vertical integrations with respect to LAI [*Chen et al.*, 2012]:

$$V_{m,\mathrm{sun}} = \frac{\int_0^{\mathrm{LAI}} V_{m,0}\chi_n N(\mathrm{LAI}) f_{sh}(\mathrm{LAI})\,\mathrm{dLAI}}{\int_0^{\mathrm{LAI}} f_{sh}(\mathrm{LAI})\,\mathrm{dLAI}} = V_{m,0}\chi_n N_0\frac{k\{1 - \exp[-(k_n + k)\,\mathrm{LAI}]\}}{(k_n + k)[1 - \exp(-k\,\mathrm{LAI})]}, \tag{A9}$$

$$V_{m,\mathrm{sh}} = \frac{\int_0^{\mathrm{LAI}} V_{m,0}\chi_n N(LAI) f_{sh}(LAI)\,\mathrm{dLAI}}{\int_0^{\mathrm{LAI}} f_{sh}(\,\mathrm{LAI})\,\mathrm{dLAI}} = V_{m,0}\chi_n N_0 \frac{\frac{1}{k_n}[1 - \exp(-k_n\,\mathrm{LAI})] - \frac{1}{k_n+k}\{1 - \exp[-(k_n+k)\,\mathrm{LAI}]\}}{\mathrm{LAI} - \frac{1}{k}[1 - \exp(-k\,\mathrm{LAI})]}, \quad \text{(A10)}$$

where $k = G(\theta)\Omega/\cos\theta$; $G(\theta)$ is the projection coefficient, usually taken as 0.5 for spherical leaf angle distribution, Ω is the clumping index, and θ is the solar zenith angle.

[56] As a result, the maximum electronic transport rates for the representative sunlit and shaded leaves are obtained as

$$J_{m,\mathrm{sun}}\left(\mathrm{or}\,J_{m,\mathrm{sh}}\right) = 29.1 + 1.6V_{m,\mathrm{sun}}\left(\mathrm{or}\,V_{m,\mathrm{sh}}\right). \quad \text{(A11)}$$

In this way, the effects of the vertical nitrogen gradient in the canopy on both the maximum carboxylation rate and the maximum electron transport rate are considered.

[57] **Acknowledgments.** This study was conducted under the auspices of the North American Carbon Program site-model intercomparison synthesis. This research was supported by the Canadian Foundation for Climate and Atmospheric Sciences (CFCAS) (GR464) and the Canadian Carbon Program (CCP), also funded by CFCAS. U.S.-Syv was funded by the Office of Science (BER), U.S. Department of Energy Terrestrial Carbon Processes program, grant DE-FG02-00ER63023. We acknowledge the agencies that supported the flux tower operations of the towers used here, which are all part of CCP and Ameriflux. We specifically acknowledge the principal investigators of each studied site and in particular Dennis Baldocchi, Alan Barr, Peter Curtis, Lianhong Gu, Tilden Meyers, David Hollinger, Russ Monson, Walter Oechel, Nigel Roulet, and Elyn Humphreys. M.S. is very thankful to A. Kreimer for immeasurable help in data processing and programming.

References

Alton, P. B. (2008), Reduced carbon sequestration in terrestrial ecosystems under overcast skies compared to clear skies, *Agric. For. Meteorol.*, *148*, 1641–1653, doi:10.1016/j.agrformet.2008.05.014.

Alton, P. B., R. Ellis, S. O. Los, and P. R. North (2007), Improved global simulations of gross primary product based on a separate and explicit treatment of diffuse and direct sunlight, *J. Geophys. Res.*, *112*, D07203, doi:10.1029/2006JD008022.

Arora, V. K. (2003), Simulating energy and carbon fluxes over winter wheat using coupled land surface and terrestrial ecosystem models, *Agric. For. Meteorol.*, *118*, 21–47, doi:10.1016/S0168-1923(03)00073-X.

Baldocchi, D. (1994), An analytical solution for coupled leaf photosynthesis and somatal conductance models, *Tree Physiol.*, *14*, 1069–1079.

Baldocchi, D. (2003), Assessing the eddy covariance technique for evaluating carbon dioxide exchange rates of ecosystems: Past, present and future, *Global Change Biol.*, *9*(4), 479–492, doi:10.1046/j.1365-2486.2003.00629.x.

Baldocchi, D. D., and P. C. Harley (1995), Scaling carbon dioxide and water vapor exchange from leaf to canopy in a deciduous forest: Model testing and application, *Plant Cell Environ.*, *18*, 1157–1173, doi:10.1111/j.1365-3040.1995.tb00626.x.

Baldocchi, D. D., and K. B. Wilson (2001), Modeling CO_2 and water vapor exchange of a temperate broadleaved forest across hourly to decadal time scales, *Ecol. Modell.*, *142*, 155–184, doi:10.1016/S0304-3800(01)00287-3.

Baldocchi, D. D., and L. Xu (2005), Carbon exchange of deciduous broadleaved forests in temperate and Mediterranean regions, in *Carbon Balance of Forest Biomes*, edited by P. J. Jarvis and H. Griffiths, pp. 187–216, BIOS Sci., Oxford, U. K.

Ball, J. T., I. E. Woodrow, and J. A. Berry (1987), A model predicting stomatal conductance and its contribution to the control of photosynthesis under different environmental conditions, in *Progress in Photosynthesis Research*, edited by J. Biggins, pp. 221–224, Martinus Nijhoff, Dordrecht, Netherlands.

Barr, A. G., T. A. Black, E. H. Hogg, N. Kljun, K. Morgenstern, and Z. Nesic (2004), Inter-annual variability in the leaf area index of a boreal aspen-hazelnut forest in relation to net ecosystem production, *Agric. For. Meteorol.*, *126*, 237–255, doi:10.1016/j.agrformet.2004.06.011.

Black, T. A., J. M. Chen, X. Lee, and R. M. Sagar (1991), Characteristics of shortwave and longwave irradiances under a Douglas-fir forest stand, *Can. J. For. Res.*, *21*, 1020–1028, doi:10.1139/x91-140.

Bonan, G. B. (1995), Land-atmosphere CO_2 exchange simulated by a land surface process model coupled to an atmospheric general circulation model, *J. Geophys. Res.*, *100*, 2817–2831, doi:10.1029/94JD02961.

Bradford, J. B., R. A. Birdsey, L. A. Joyce, and M. G. Ryan (2008), Tree age, disturbance history, and carbon stocks and fluxes in subalpine Rocky Mountain forests, *Global Change Biol.*, *14*(12), 2882–2897, doi:10.1111/j.1365-2486.2008.01686.x.

Carswell, F. E., P. Meir, E. V. Wandelli, L. C. M. Bonates, B. Kruijt, E. M. Barbosa, A. D. Nobre, J. Grace, and P. G. Jarvis (2000), Photosynthetic capacity in a central Amazonian rain forest, *Tree Physiol.*, *20*(3), 179–186, doi:10.1093/treephys/20.3.179.

Chen, B., J. M. Chen, G. Mo, K. Yuan, K. Higuchi, and D. Chan (2007), Modeling and scaling coupled energy, water, and carbon fluxes based on remote sensing: An application to Canada's landmass, *J. Hydrometeorol.*, *8*, 123–143, doi:10.1175/JHM566.1.

Chen, J. M. (1996), Optically based methods for measuring seasonal variation in leaf area index of boreal conifer forests, *Agric. For. Meteorol.*, *80*, 135–163, doi:10.1016/0168-1923(95)02291-0.

Chen, J. M., and S. Leblanc (1997), A 4-scale bidirectional reflection model based on canopy architecture. *IEEE Trans. Geosci. Remote Sens.*, *35*, 1316–1337, doi:10.1109/36.628798.

Chen, J. M., P. M. Rich, T. S. Gower, J. M. Norman, and S. Plummer (1997), Leaf area index of boreal forests: Theory, techniques and measurements, *J. Geophys. Res.*, *102*, 29,429–29,444, doi:10.1029/97JD01107.

Chen, J. M., J. Liu, J. Cihlar, and M. L. Goulden (1999), Daily canopy photosynthesis model through temporal and spatial scaling for remote sensing applications, *Ecol. Modell.*, *124*, 99–119, doi:10.1016/S0304-3800(99)00156-8.

Chen, J. M., et al. (2002), Derivation and validation of Canada-wide coarse-resolution leaf area index maps using high-resolution satellite imagery and ground measurements, *Remote Sens. Environ.*, *80*, 165–184.

Chen, J. M., J. Liu, S. G. Leblanc, R. Lacaze, and J.-L. Roujean (2003), Multi-angular optical remote sensing for assessing vegetation structure and carbon absorption, *Remote Sens. Environ.*, *84*, 516–525, doi:10.1016/S0034-4257(02)00150-5.

Chen, J. M., C. H. Menges, and S. G. Leblanc (2005), Global derivation of the vegetation clumping index from multi-angular satellite data, *Remote Sens. Environ.*, *97*, 447–457, doi:10.1016/j.rse.2005.05.003.

Chen, J. M., G. Mo, J. Pisek, J. Liu, F. Deng, M. Ishizawa, and D. Chan (2012), Effects of foliage clumping on the estimation of global terrestrial gross primary productivity, *Global Biogeochem. Cycles*, doi:10.1029/2010GB003996, in press.

Chen, Q., D. Baldocchi, P. Gong, and T. Dawson (2008), Modeling radiation and photosynthesis of a heterogeneous savanna woodland landscape with a hierarchy of model complexities, *Agric. For. Meteorol.*, *148*, 1005–1020, doi:10.1016/j.agrformet.2008.01.020.

Dai, Y., R. E. Dickinson, and Y.-P. Wang (2004), A two-big-leaf model for canopy temperature, photosynthesis, and stomatal conductance, *J. Clim.*, *17*, 2281–2299, doi:10.1175/1520-0442(2004)017<2281:ATMFCT>2.0.CO;2.

Deng, F., J. M. Chen, S. Plummer, M. Chen, and J. Pisek (2006), Algorithm for global leaf area index retrieval using satellite imagery, *IEEE Trans. Geosci. Remote Sens.*, *44*(11), 2219–2229, doi:10.1109/TGRS.2006.872100.

de Pury, D. G. G., and G. D. Farquhar (1997), Simple scaling of photosynthesis from leaves to canopy without the errors of big-leaf models, *Plant Cell Environ.*, *20*, 537–557, doi:10.1111/j.1365-3040.1997.00094.x.

Desai, A. R., P. V. Bolstad, B. D. Cook, K. J. Davis, and E. V. Carey (2005), Comparing net ecosystem exchange of carbon dioxide between an old-growth and mature forest in the upper midwest, USA, *Agric. For. Meteorol.*, *128*(1–2), 33–55, doi:10.1016/j.agrformet.2004.09.005.

Desai, A. R., et al. (2008), Cross site evaluation of eddy covariance GPP and RE decomposition techniques, *Agric. For. Meteorol.*, *148*(6–7), 821–838, doi:10.1016/j.agrformet.2007.11.012.

Epstein, H. E., M. P. Calef, M. D. Walker, F. S. Chapin, and A. M. Starfield (2004), Detecting changes in arctic tundra plant communities in response to warming over decadal time scales, *Global Change Biol.*, *10*(8), 1325–1334, doi:10.1111/j.1529-8817.2003.00810.x.

Erbs, D. G., S. A. Klein, and J. A. Duffie (1982), Estimation of diffuse radiation fraction for hourly, daily and monthly average global radiation, *Sol. Energy*, *28*, 293–302, doi:10.1016/0038-092X(82)90302-4.

Farquhar, G. D. (1989), Models of integrated photosynthesis of cells and leaves, *Philos. Trans. R. Soc. London B*, *323*, 357–367, doi:10.1098/rstb.1989.0016.

Farquhar, G. D., and S. von Caemmerer (1982), Modelling of photosynthetic response to environmental conditions, in *Encyclopedia of Plant Physiology*, vol. 12B, edited by O. L. Lange et al., pp.549–587, Springer-Verlag, Berlin.

Farquhar, G. D., S. von Caemmerer, and J. A. Berry (1980), A biochemical model of photosynthetic CO_2 assimilation in leaves of C3 species, *Planta*, *149*, 78–90, doi:10.1007/BF00386231.

Feng, X., G. Liu, J. M. Chen, M. Chen, J. Liu, W. Ju, R. Sun, and W. Zhou (2007), Simulating net primary productivity of terrestrial ecosystems in China using a process model driven by remote sensing, *J. Environ. Manage.*, *85*, 563–573, doi:10.1016/j.jenvman.2006.09.021.

Field, C. B. (1983), Allocating leaf nitrogen for the maximization of carbon gain: Leaf age as a control on the allocation program, *Oecologia*, *56*, 341–347, doi:10.1007/BF00379710.

Flexas, J., M. Ribas-Carbo, A. Diaz-Espejo, J. Galmes, and H. Medrano (2008), Mesophyll conductance to CO_2: Current knowledge and future prospects, *Plant Cell Environ.*, *31*, 602–621, doi:10.1111/j.1365-3040.2007.01757.x.

Friend, A. D. (2001), Modeling canopy CO_2 fluxes: Are 'big-leaf' simplifications justified? *Global Ecol. Biogeogr.*, *10*, 603–619, doi:10.1046/j.1466-822x.2001.00268.x.

Friend, A. D., A. K. Stevens, R. G. Knox, and M. G. R. Cannell (1997), A process- based, terrestrial biosphere model of ecosystem dynamics (Hybrid v3.0), *Ecol. Modell.*, *95*, 249–287, doi:10.1016/S0304-3800(96)00034-8.

Frolking, S. E., et al. (1998), Relationship between ecosystem productivity and photosynthetically active radiation for northern peatlands, *Global Biogeochem. Cycles*, *12*, 115–126, doi:10.1029/97GB03367.

Gough, C. M., C. S. Vogel, H. P. Schmid, H.-B. Su, and P. S. Curtis (2008), Multi-year convergence of biometric and meteorological estimates of forest carbon storage, *Agric. For. Meteorol.*, *148*, 158–170, doi:10.1016/j.agrformet.2007.08.004.

Groenendijk, M., et al. (2010), Assessing parameter variability in a photosynthesis model within and between plant functional types using global Fluxnet eddy covariance data, *Agric. For. Meteorol.*, *151*, 22–38, doi:10.1016/j.agrformet.2010.08.013.

Gu, L., D. D. Baldocchi, S. B. Verma, T. A. Black, T. Vesala, E. M. Falge, and P. R. Dowty (2002), Superiority of diffuse radiation for terrestrial ecosystem productivity, *J. Geophys. Res.*, *107*(D6), 4050, doi:10.1029/2001JD001242.

Gu, L., T. Meyers, S. G. Pallardy, P. J. Hanson, B. Yang, M. Heuer, K. P. Hosman, J. S. Riggs, D. Sluss, and S. D. Wullschleger (2006), Direct and indirect effects of atmospheric conditions and soil moisture on surface energy partitioning revealed by a prolonged drought at a temperate forest site, *J. Geophys. Res.*, *111*, D16102, doi:10.1029/2006JD007161.

Houborg, R., M. C. Anderson, J. M. Norman, T. Wilson, and T. Meyers (2009), Intercomparison of a "bottom-up" and "top-down" modeling paradigm for estimating carbon and energy fluxes over a variety of vegetative regimes across the US, *Agric. For. Meteorol.*, *149*, 1875–1895, doi:10.1016/j.agrformet.2009.06.014.

Ingestad, T., and A.-B. Lund (1986), Theory and techniques for steady state mineral nutrition and growth of plants, *Scand. J. For. Res.*, *1*, 439–453, doi:10.1080/02827588609382436.

Jarvis, P., J. Massheder, S. Hale, J. Moncrieff, M. Rayment, and S. Scott (1997), Seasonal variation of carbon dioxide, water vapor, and energy exchanges of a boreal black spruce forest, *J. Geophys. Res.*, *102*, 28,953–28,966, doi:10.1029/97JD01176.

Jogireddy, V. R. (2004), *Carbon Assimilation and Modeling of the European Land Surface (CAMELS)*, Hadley Centre for Climate Pred. and Res., Exeter, U. K.

Ju, W., J. M. Chen, T. A. Black, A. G. Barr, J. Liu, and B. Chen (2006), Modeling multi-year coupled carbon and water fluxes in a boreal aspen forest, *Agric. For. Meteorol.*, *140*, 136–151, doi:10.1016/j.agrformet.2006.08.008.

Kattge, J., W. Knorr, T. Raddatz, and C. Wirth (2009), Quantifying photosynthetic capacity and its relationship to leaf nitrogen content for global scale terrestrial biosphere models, *Global Change Biol.*, *15*, 976–991, doi:10.1111/j.1365-2486.2008.01744.x.

Kotchenova, S. Y., X. Song, N. V. Shabanov, C. S. Potter, Y. Knyazikhin, and R. B. Myneni (2004), Lidar remote sensing for modeling gross primary production of deciduous forests, *Remote Sens. Environ.*, *92*, 158–172, doi:10.1016/j.rse.2004.05.010.

Kull, O. (2002), Acclimation of photosynthesis in canopies: Models and limitations, *Oecologia*, *133*, 267–279, doi:10.1007/s00442-002-1042-1.

Kull, O., and P. G. Jarvis (1995), The role of nitrogen in a simple scheme to scale up photosynthesis from leaf to canopy, *Plant Cell Environ.*, *18*, 1174–1182, doi:10.1111/j.1365-3040.1995.tb00627.x.

Lai, C.-T., G. Katul, R. Oren, D. Ellsworth, and K. Shafer (2000), Modeling CO_2 and water vapor turbulent flux distributions within a forest canopy, *J. Geophys. Res.*, *105*, 26,333–26,351, doi:10.1029/2000JD900468.

Leuning, R. (1995), A critical appraisal of a combined stomatal-photosynthesis model for C3 plants, *Plant Cell Environ.*, *18*, 339–355, doi:10.1111/j.1365-3040.1995.tb00370.x.

Leuning, R. (1997), Scaling to a common temperature improves the correlation between photosynthesis parameters J_{max} and V_{cmax}, *J. Exp. Bot.*, *48*, 345–347, doi:10.1093/jxb/48.2.345.

Liu, J., J. M. Chen, J. Cihlar, and W. M. Park (1997), A process-based boreal ecosystem productivity simulator using remote sensing inputs, *Remote Sens. Environ.*, *62*, 158–175, doi:10.1016/S0034-4257(97)00089-8.

Liu, J., J. M. Chen, J. Cihlar, and W. Chen (1999), Net primary productivity distribution in the BOREAS region from a process model using satellite and surface data, *J. Geophys. Res.*, *104*, 27,735–27,754, doi:10.1029/1999JD900768.

Liu, J., J. M. Chen, J. Cihlar, and W. Chen (2002), Net primary productivity mapped for Canada at 1-km resolution, *Global Ecol. Biogeogr.*, *11*, 115–129, doi:10.1046/j.1466-822X.2002.00278.x.

Lloyd, J., J. Grace, A. C. Miranda, P. Meir, S. C. Wong, B. S. Miranda, I. R. Wright, J. H. C. Gash, and J. McIntyre (1995), A simple calibrated model of Amazon rainforest productivity based on leaf biochemical properties, *Plant Cell Environ.*, *18*(10), 1129–1145, doi:10.1111/j.1365-3040.1995.tb00624.x.

Medlyn, B. E., et al. (1999a), Effects of elevated [CO_2] on photosynthesis in European forest species: A meta-analysis of model parameters, *Plant Cell Environ.*, *22*, 1475–1495, doi:10.1046/j.1365-3040.1999.00523.x.

Medlyn, B., et al. (1999b), Meta-analysis of model parameters, in *Predicted Impacts of Rising Carbon Dioxide and Temperature on Forests in Europe at Stand Scale*, *ECOCRAFT Environment R&D Rep., ENV4–CT95–0077 IC20–CT96–0028*, Univ. of Edinburgh, Edinburgh, U. K.

Meir, P., B. Kruijt, M. Broadmeadow, E. Barbosa, O. Kull, F. Carswell, A. Nobre, and P. Jarvis (2002), Acclimation of photosynthetic capacity to irradiance in tree canopies in relation to leaf nitrogen concentration and leaf mass per unit area, *Plant Cell Environ.*, *25*, 343–357, doi:10.1046/j.0016-8025.2001.00811.x.

Mercado, L., J. Lloyd, F. Carswell, Y. Malhi, P. Meir, and A. D. Nobre (2006), Modelling Amazonian forest eddy covariance data: A comparison of big-leaf versus sun/shade models for the C-14 tower at Manaus I. Canopy photosynthesis, *Acta Amazon.*, *36*(1), 69–82, doi:10.1590/S0044-59672006000100009.

Mercado, L., C. Huntingford, J. H. C. Gash, P. M. Cox, and V. Jogireddy (2007), Improving the representation of radiation interception and photosynthesis for climate model applications, *Tellus*, *59B*, 553–565.

Monteith, J. L. (1972), Solar radiation and productivity in tropical ecosystem, *J. Appl. Ecol.*, *9*, 747–766, doi:10.2307/2401901.

Monteith, J. L. (1973), *Principles of Environmental Physics*, Edward Arnold, London.

Moran, M. S., A. F. Rahman, J. C. Washburne, D. C. Goodrich, M. A. Weltz, and W. P. Kustas (1996), Combining the Penman-Monteith equation with measurements of surface temperature and reflectance to estimate evaporation rates of semiarid grassland, *Agric. For. Meteorol.*, *80*, 87–109, doi:10.1016/0168-1923(95)02292-9.

Norman, J. M. (1980), Interfacing leaf and canopy light interception models, in *Predicting Photosynthesis for Ecosystem Models*, edited by J. D. Hesketh and J. W. Jones, pp. 49–67, CRC Press, Boca Raton, Fla.

Norman, J. M. (1982), Simulation of microclimates, in *Biometeorology in Integrated Pest Management*, edited by J. L. Hatfield and I. J. Thomason, pp. 65–99, Academic, San Diego, Calif.

Op de Beeck, M., B. Gielen, I. Jonckheere, R. Samson, I. A. Janssens, and R. Ceulemans (2009), Needle age-related and seasonal photosynthetic capacity variation is negligible for modelling yearly gas exchange of a temperate Scots pine forest, *Biogeosci. Discuss.*, *6*, 9737–9780, doi:10.5194/bgd-6-9737-2009.

Piel, C., E. Frak, X. Le Roux, and B. Genty (2002), Effect of local irradiance on CO_2 transfer conductance of mesophyll in walnut, *J. Exp. Bot.*, *53*(379), 2423–2430, doi:10.1093/jxb/erf095.

Rastetter, E. B., A. W. King, B. J. Cosby, G. M. Hornberger, R. V. O'Neill, and J. E. Hobbie (1992), Aggregating fine-scale ecological knowledge to model coarser-scale attributes of ecosystems, *Ecol. Appl.*, *2*, 55–70, doi:10.2307/1941889.

Raupach, M. R., and J. J. Finnigan (1988), Single-layer models of evaporation from plant canopies are incorrect but useful, whereas multilayer

models are correct but useless: Discuss, *Aust. J. Plant Physiol.*, *15*, 705–716, doi:10.1071/PP9880705.

Samson, R., and R. Lemeur (2001), Energy balance storage terms and big-leaf evapotranspiration in a mixed deciduous forest, *Ann. For. Sci.*, *58*, 529–541, doi:10.1051/forest:2001143.

Schwalm, C., et al. (2010), A model-data intercomparison of CO_2 exchange across North America: Results from the North American Carbon Program site synthesis, *J. Geophys. Res.*, *115*, G00H05, doi:10.1029/2009JG001229.

Sellers, P. J., J. A. Berry, G. J. Collatz, C. B. Field, and F. G. Hall (1992), Canopy reflectance, photosynthesis and transpiration. III. A reanalysis using improved leaf models and a new canopy integration scheme, *Remote Sens. Environ.*, *42*, 187–216, doi:10.1016/0034-4257(92)90102-P.

Sinclair, T. R., C. E. Murphy, and K. R. Knoerr (1976), Development and evaluation of simplified models for simulating canopy photosynthesis and transpiration, *J. Appl. Ecol.*, *13*(3), 813–829, doi:10.2307/2402257.

Spitters, C. J. T. (1986), Separating the diffuse and direct component of global radiation and its implications for modeling canopy photosynthesis. Part II. Calculation of canopy photosynthesis, *Agric. For. Meteorol.*, *38*, 231–242, doi:10.1016/0168-1923(86)90061-4.

Šprtová, M., and M. V. Marek (1999), Response of photosynthesis to radiation and intercellular CO_2 concentration in sun and shade shoots of Norway spruce, *Photosynthetica*, *37*, 433–445, doi:10.1023/A:1007111911415.

Thornton, P. E., S. W. Running, and M. A. White (1997), Generating surfaces of daily meteorological variables over large regions of complex terrain, *J. Hydrol.*, *190*, 214–251, doi:10.1016/S0022-1694(96)03128-9.

Wang, Q., J. Tenhunen, E. Falge, C. Bernhofer, A. Granier, and T. Vesalas (2004), Simulation and scaling of temporal variation in gross primary production for coniferous and deciduous temperate forests, *Global Change Biol.*, *10*, 37–51, doi:10.1111/j.1365-2486.2003.00716.x.

Wang, Y.-P., and R. Leuning (1998), A two-leaf model for canopy conductance, photosynthesis and partitioning of available energy: I. Model description and comparison with a multi-layered model, *Agric. For. Meteorol.*, *91*, 89–111, doi:10.1016/S0168-1923(98)00061-6.

Warren, C. R. (2008), Stand aside stomata, another actor deserves centre stage: The forgotten role of the internal conductance to CO_2 transfer, *J. Exp. Bot.*, *59*(7), 1475–1487, doi:10.1093/jxb/erm245.

Weiss, A., and J. M. Norman (1985), Partitioning solar radiation into direct and diffuse, visible and near-infrared components, *Agric. For. Meteorol.*, *34*, 205–213, doi:10.1016/0168-1923(85)90020-6.

Weiß, M., and L. Menzel (2008), A global comparison of four potential evapotranspiration equations and their relevance to stream flow modelling in semi-arid environments, *Adv. Geosci.*, *18*, 15–23, doi:10.5194/adgeo-18-15-2008.

Wolf, A., K. Akshalov, N. Saliendra, D. A. Johnson, and E. A. Laca (2006), Inverse estimation of Vc_{max}, leaf area index, and the Ball-Berry parameter from carbon and energy fluxes, *J. Geophys. Res.*, *111*, D08S08, doi:10.1029/2005JD005927.

Wullschleger, S. D. (1993), Biochemical limitations to carbon assimilation in C3 plants–A retrospective analysis of the A/Ci curves from 109 species, *J. Exp. Bot.*, *44*, 907–920, doi:10.1093/jxb/44.5.907.

Xiao, X. M., Q. Y. Zhang, D. Hollinger, J. Aber, and B. Moore (2005), Modeling gross primary production of an evergreen needleleaf forest using MODIS and climate data, *Ecol. Appl.*, *15*(3), 954–969, doi:10.1890/04-0470.

Xu, L. K., and D. D. Baldocchi (2003), Seasonal trends in photosynthetic parameters and stomatal conductance of blue oak (*Quercus douglasii*) under prolonged summer drought and high temperature, *Tree Physiol.*, *23*, 865–877.

Zhou, Y., Q. Zhu, J. M. Chen, Y. Q. Wang, J. Liu, R. Sun, and S. Tang (2007), Observation and simulation of net primary productivity in Qilian Mountain, Western China, *J. Environ. Manage.*, *85*, 574–584, doi:10.1016/j.jenvman.2006.04.024.

J. M. Chen, Department of Geography, University of Toronto, 100 St. George St., Toronto, ON M5S 3 G3, Canada.

A. Desai, Center for Climatic Research, Nelson Institute for Environmental Studies, University of Wisconsin – Madison, AOSS 1549, 1225 W. Dayton St., Madison, WI 53706, USA.

C. M. Gough, Department of Biology, Virginia Commonwealth University, Box 842012, 1000 W. Cary St., Richmond, VA 23284-2012, USA.

M. Sprintsin, Institute of Agricultural Engineering, Agricultural Research Organization Volcani Centre, P.O. Box 6, Bet Dagan 50250, Israel. (misprin@gmail.com)